Supplementary Information (SI) for Dalton Transactions.
This journal is © The Royal Society of Chemistry 2025

Supplementary Information

Lysosome-targeted Ru(II)-cyclopentadienyl organometallic anticancer complexes

Ricardo G. Teixeira[a,§], Lívia Stenico[b], Xavier Fontrodona[c], Isabel Romero[c], Radosław Starosta[a,d], Maria João Moreno[c,e], Ana Isabel Tomaz[a], Lígia C. Gomes-da-Silva[c,e,*], Andreia Valente[a,*]

[a] Centro de Química Estrutural, Institute of Molecular Sciences, Departamento de Química e Bioquímica, Faculdade de Ciências, Universidade de Lisboa, Campo Grande, 1749-016 Lisboa, Portugal

[b] Coimbra Chemistry Center – Institute of Molecular Sciences (CQC-IMS), University of Coimbra, 3004-535 Coimbra, Portugal

[c] Departament de Química and Serveis Tècnics de Recerca, Universitat de Girona, C/ M. Aurèlia Campmany, 69, E-17003 Girona, Spain

[d] Faculty of Chemistry, University of Wrocław, F. Joliot-Curie 14, 50-383, Wrocław, Poland

[e] Department of Chemistry, University of Coimbra, 3004-535 Coimbra, Portugal

[§] Current address for Ricardo G. Teixeira: Centro de Química Estrutural, Institute of Molecular Sciences, Instituto Superior Técnico, Universidade de Lisboa, Av. Rovisco Pais 1, 1049-001 Lisboa, Portugal; and Associação do Instituto Superior Técnico para a Investigação e Desenvolvimento (IST-ID), Avenida António José de Almeida 12, 1000-043 Lisboa Portugal

Corresponding authors

*E-mail: amvalente@ciencias.ulisboa.pt ; ligia.silva@uc.pt

Table of contents

Synthesis

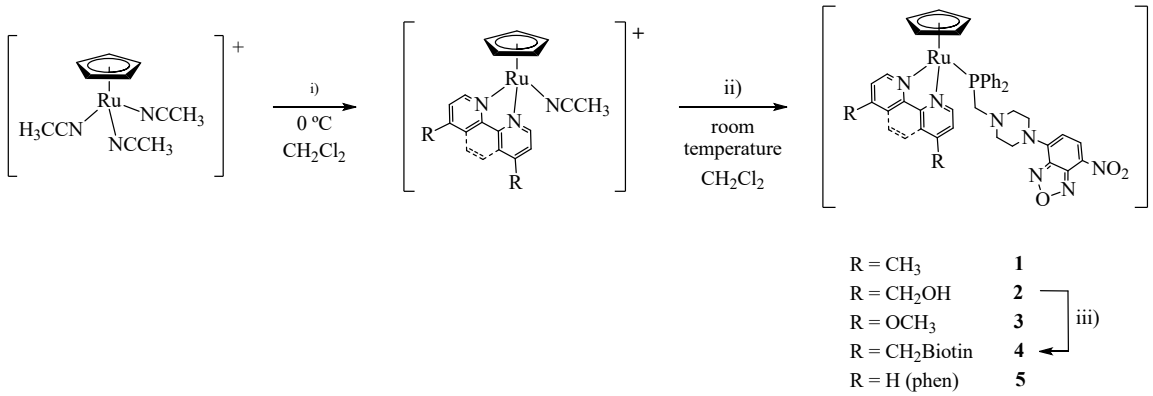

Scheme S1. Synthesis of complexes **1**–**5**; all complexes were isolated as hexafluorophosphate salts. i) 4,4'-R-2,2'-bipyridine (R = CH_3 (**1**), CH_2OH (**2**), OCH_3 (**3**)), 0ºC → room temperature, 2 h; ii) 4-(4-((diphenylphosphino)methyl)piperazin-1-yl)-7-nitrobenzo[*c*][1,2,5]oxadiazole (Ph_2P-CH_2-pip-NBD), room temperature, 4-6 h; iii) Biotin, EDC•Cl, DMAP, DMF, room temperature, overnight.

S1. NMR spectra

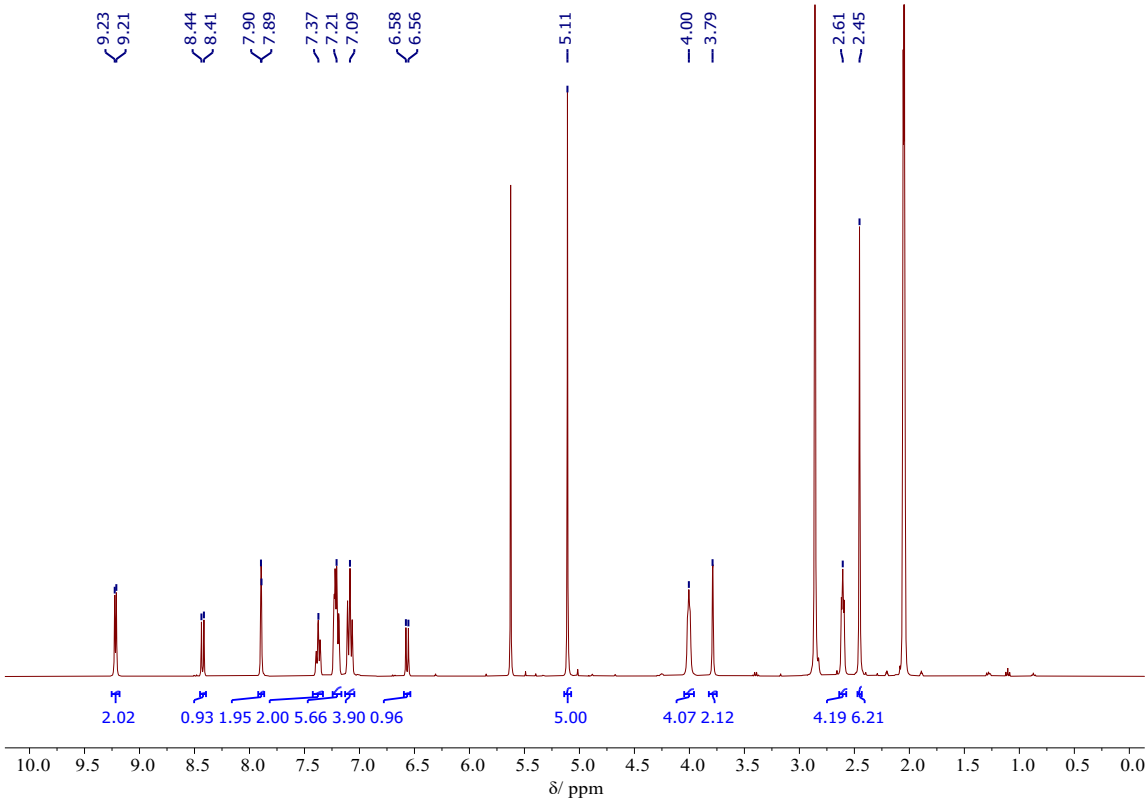

Figure S1. ^{1}H-NMR spectrum of complex **1** in acetone-d_6 at 298 K.

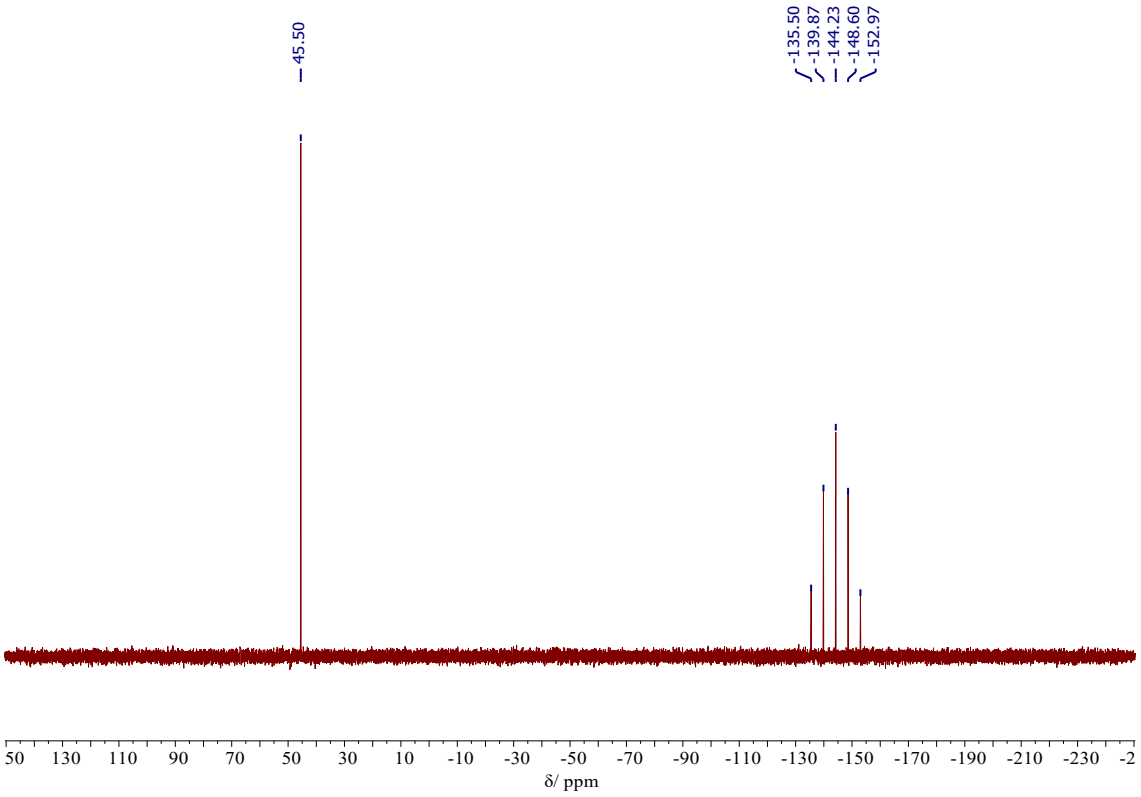

Figure S2. $^{31}P\{^{1}H\}$-NMR spectrum of complex **1** in acetone-d_6 at 298 K.

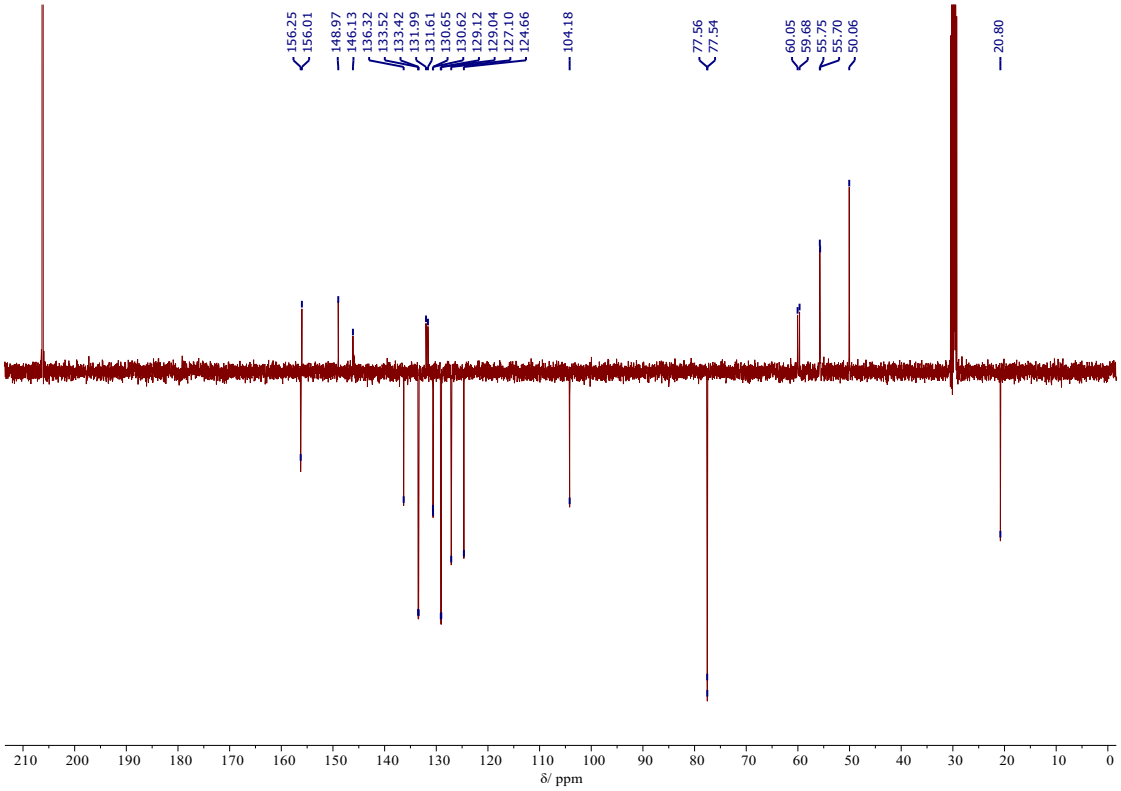

Figure S3. APT $^{13}C\{^{1}H\}$-NMR spectrum of complex **1** in acetone-d_6 at 298 K.

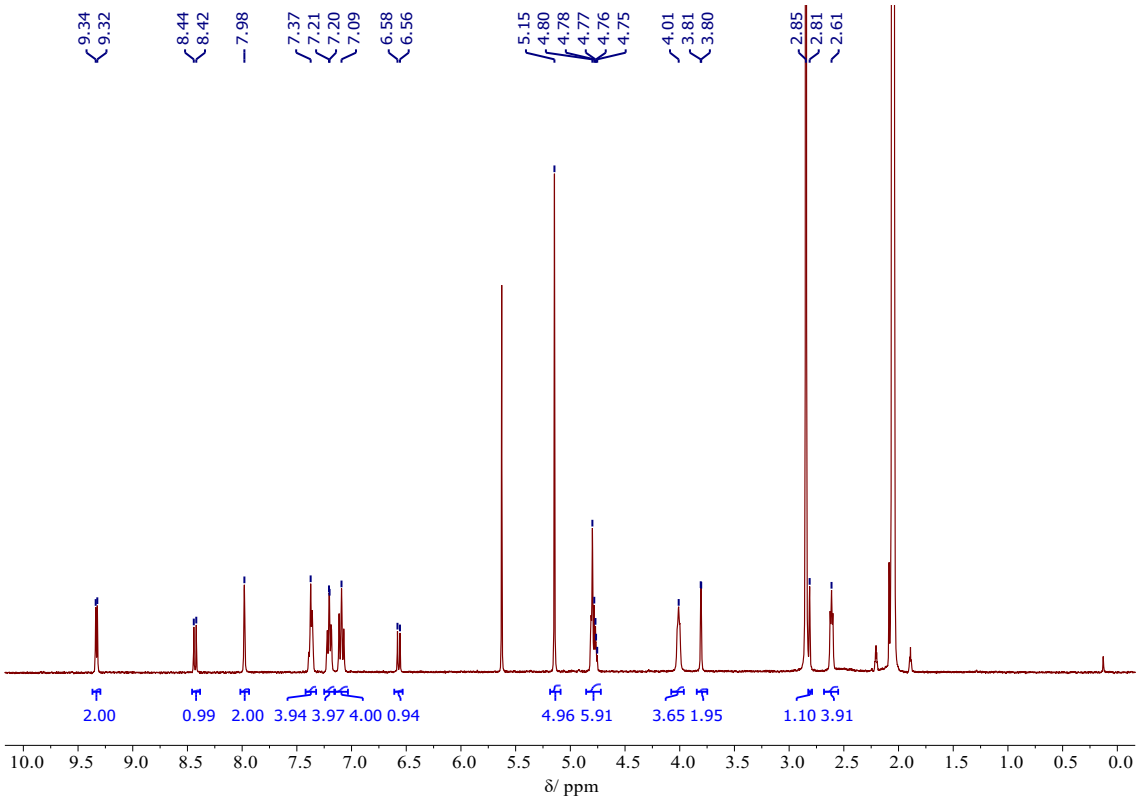

Figure S4. ^{1}H-NMR spectrum of complex **2** in acetone-d_6 at 298 K.

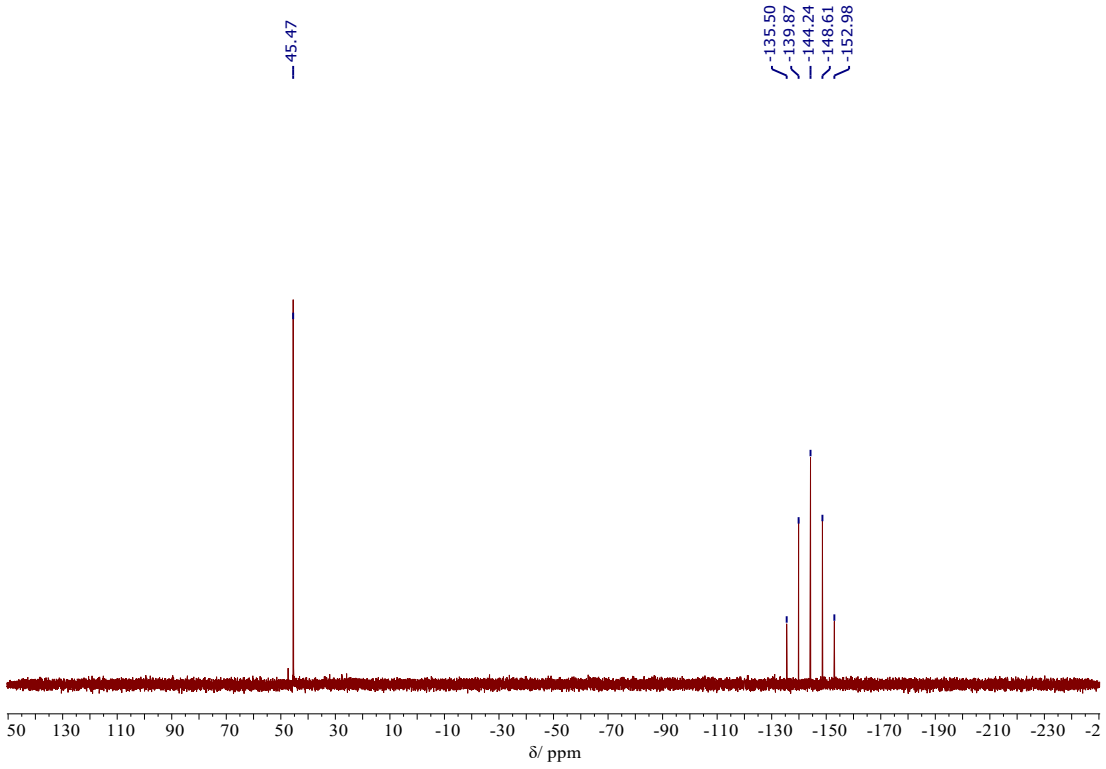

Figure S5. ^{31}P{^{1}H}-NMR spectrum of complex **2** in acetone-d_6 at 298 K.

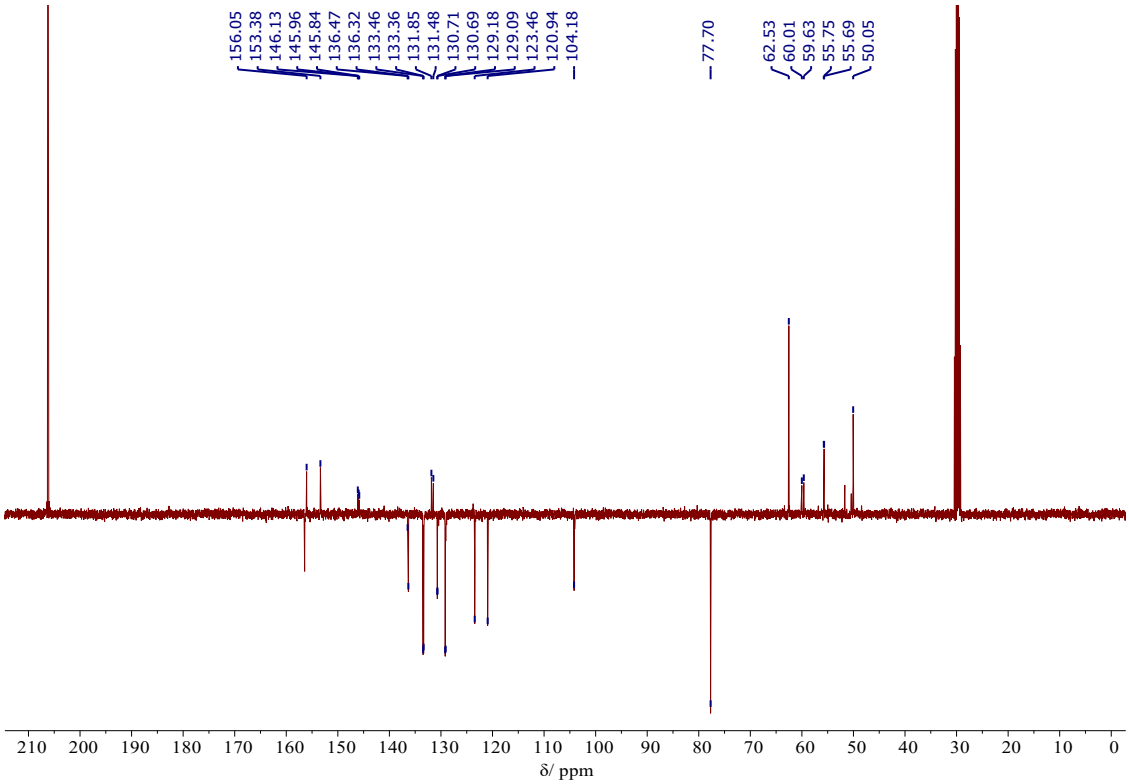

Figure S6. APT $^{13}C\{^{1}H\}$-NMR spectrum of complex **2** in acetone-d_6 at 298 K.

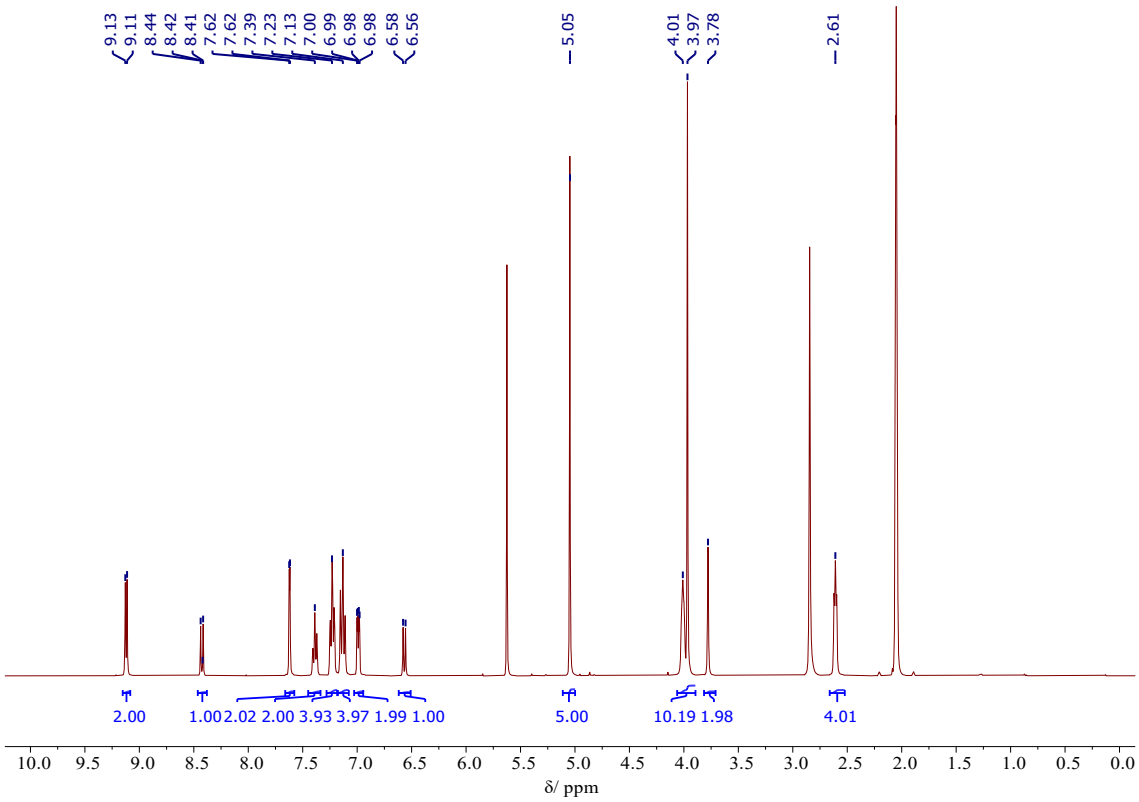

Figure S7. ^{1}H-NMR spectrum of complex **3** in acetone-d_6 at 298 K.

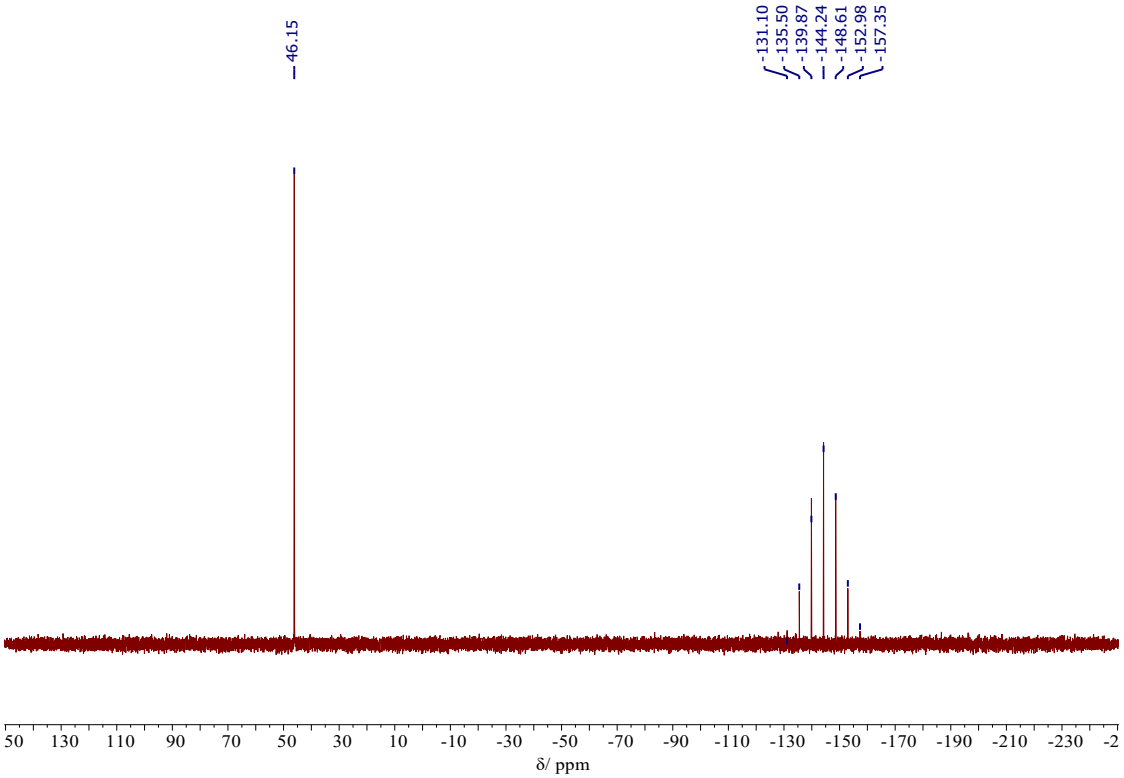

Figure S8. $^{31}P\{^{1}H\}$-NMR spectrum of complex **3** in acetone-d_6 at 298 K.

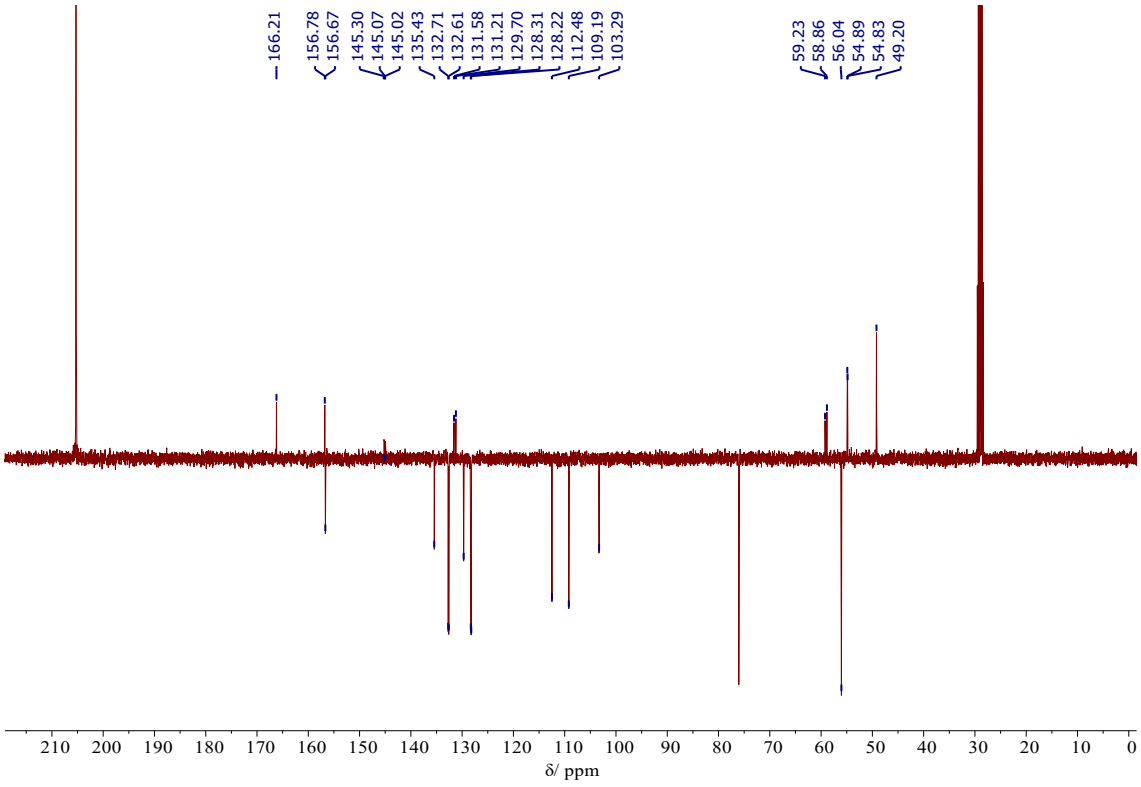

Figure S9. APT $^{13}C\{^{1}H\}$-NMR spectrum of complex **3** in acetone-d_6 at 298 K.

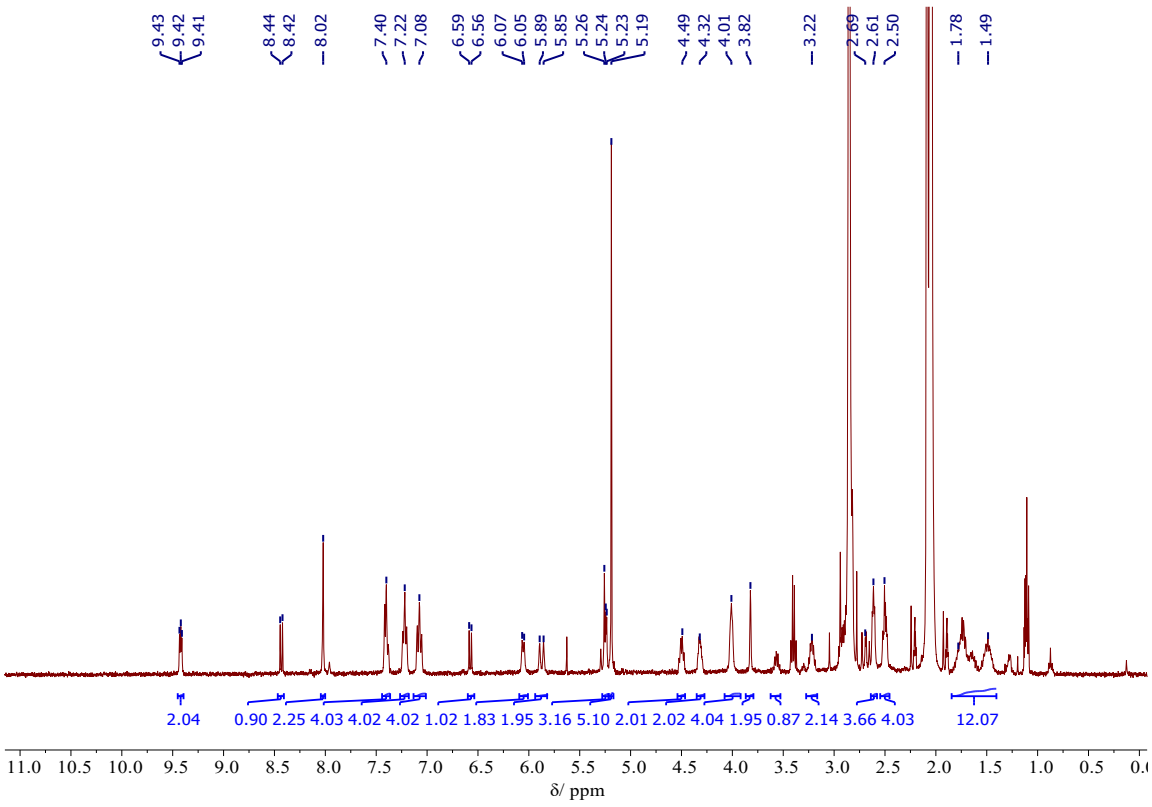

Figure S10. ^{1}H-NMR spectrum of complex **4** in acetone-d_6 at 298 K.

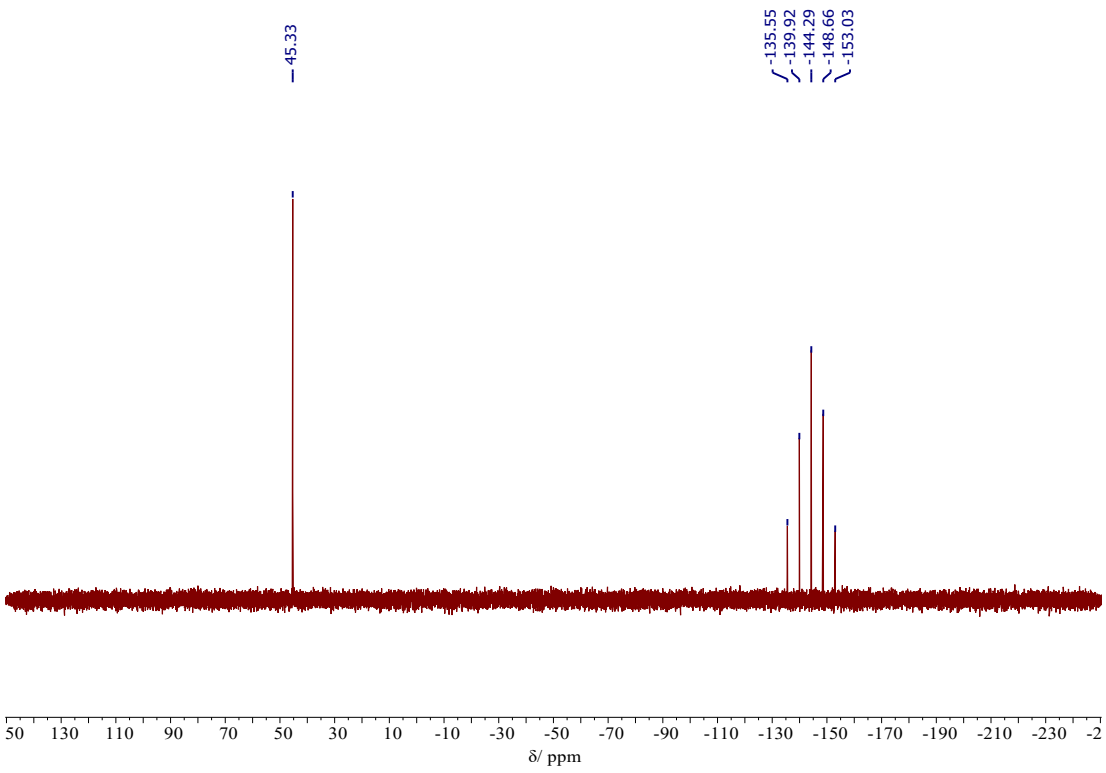

Figure S11. ^{31}P{^{1}H}-NMR spectrum of complex **4** in acetone-d$_6$ at 298 K.

74

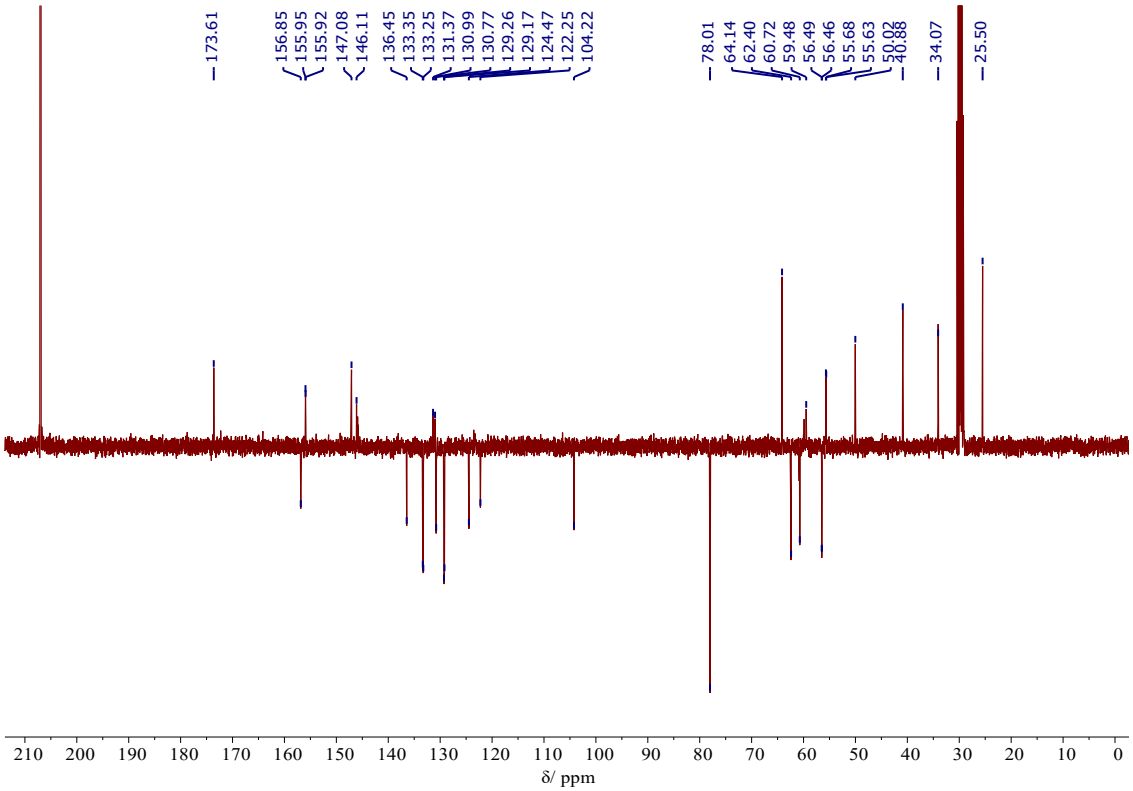

75

76 **Figure S12.** APT $^{13}C\{^{1}H\}$-NMR spectrum of complex **4** in acetone-d_6 at 298 K.

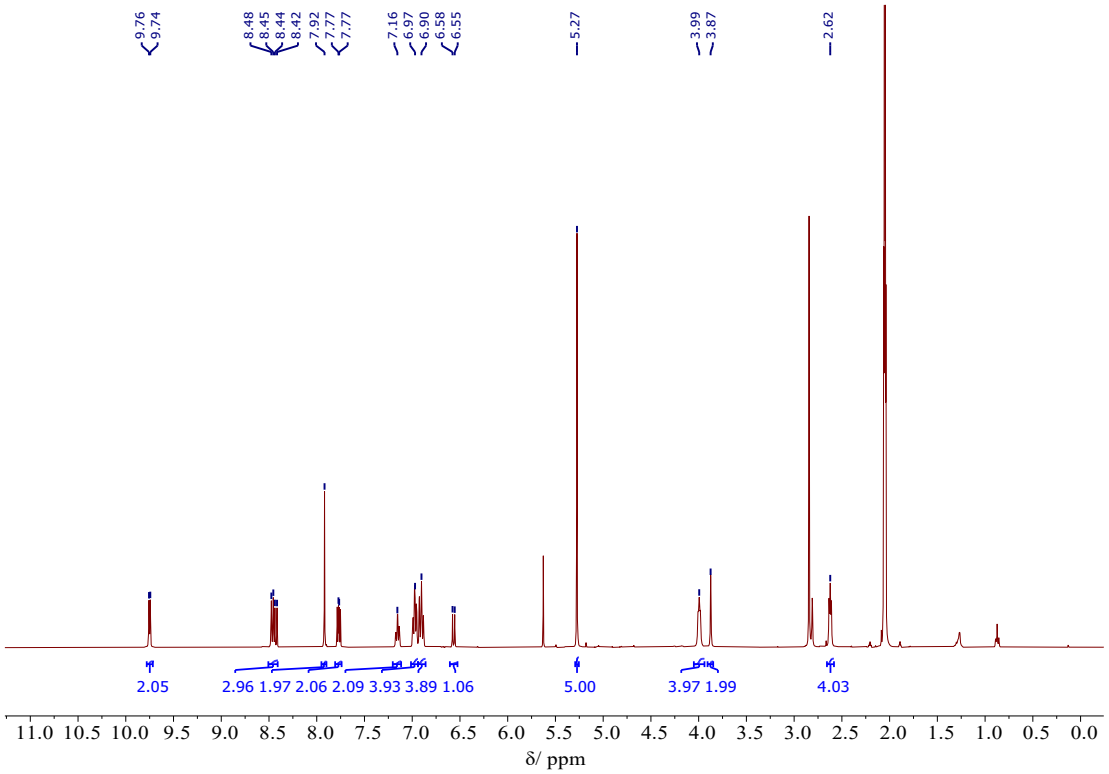

77

78 **Figure S13.** ^{1}H-NMR spectrum of complex **5** in acetone-d_6 at 298 K.

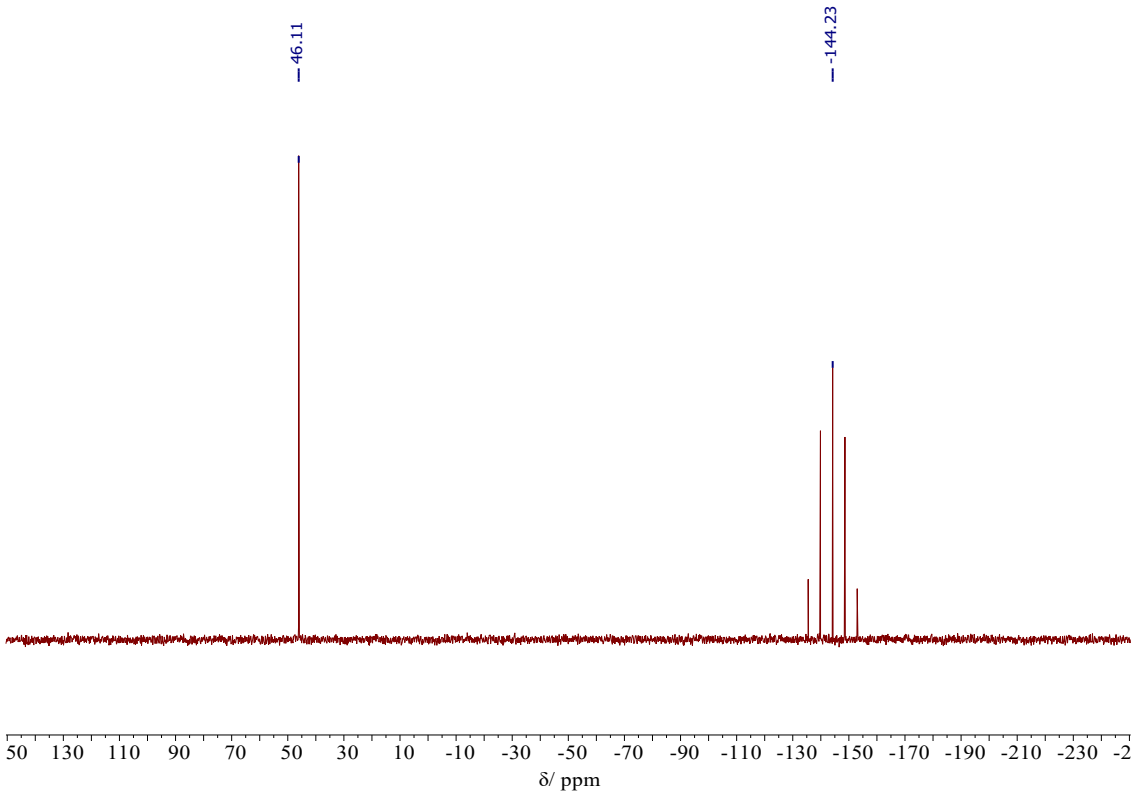

Figure S14. $^{31}P\{^{1}H\}$-NMR spectrum of complex **5** in acetone-d_6 at 298 K.

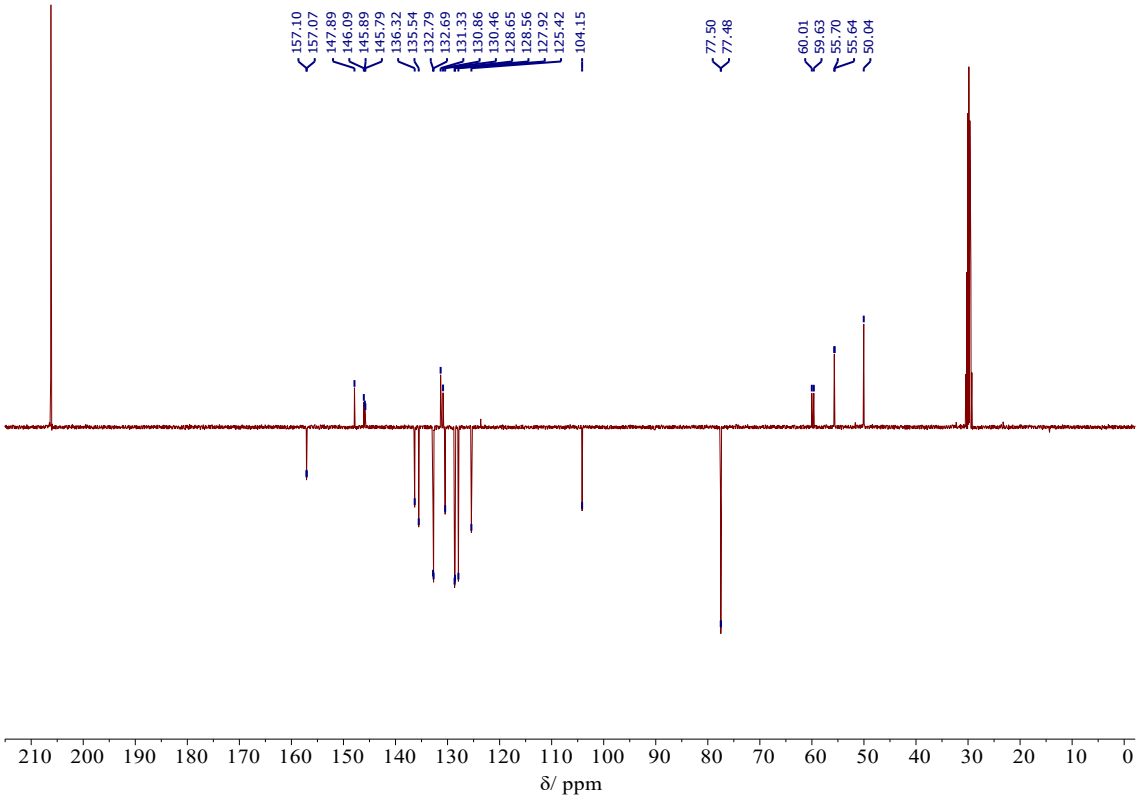

Figure S15. APT $^{13}C\{^{1}H\}$-NMR spectrum of complex **5** in acetone-d_6 at 298 K.

S2. Photophysical characterization

Table S1. Photophysical data for complexes **1**–**5** and Ph_2P-CH_2-pip-NBD ligand. Fluorescence quantum yield (ϕ_F) obtained for Ph_2P-CH_2-pip-NBD and compounds **1**–**5** in dimethylsulfoxide (DMSO) (results are from two independent experiments). λ_{abs} absorption maximum, λ_{em} emission maximum, Φ_F luminescence quantum yield, n.d. not determined, sh, shoulder

Compound	**Solvent**	**Absorbance** λ_{abs}, nm (ε, $M^{-1}cm^{-1}$)	**Emission** $\lambda_{em,}$ nm	ϕ_F
1	MeCN	238 (sh), 290 (4.3 x 10^3), 340 (2.9 x 10^3), 481	n.d.	n.d.

		(5.8 x 10^3)		
	DMSO	347.5 (1.26 x 10^4), 492 (2.49 x 10^4)	546	0.0027 ± 0.0006
2	MeCN	238 (sh), 290 (4.1 x 10^3), 339 (2.6 x 10^3), 480 (5.1 x 10^3)	n.d.	n.d.
	DMSO	346.5 (1.20 x 10^4), 492 (2.31 x 10^4)	549	0.0010 ± 0.0001
3	MeCN	236 (sh), 291 (4.7 x 10^3), 340 (2.7 x 10^3), 480 (5.6 x 10^3)	n.d.	n.d.
	DMSO	346.5 (1.31 x 10^4), 492.5 (2.53 x 10^4)	541	0.0017 ± 0.0002
4	MeCN	240 (sh), 290 (4.2 x 10^3), 340 (1.9 x 10^3), 480 (5.1 x 10^3)	n.d.	n.d.
	DMSO	346.5 (1.18 x 10^4), 491 (2.06 x 10^4)	548	0.0015 ± 0.0001
5	MeCN	239 (sh), 290 (4.3 x 10^3), 339 (2.9 x 10^3), 482 (5.6 x 10^3)	n.d.	n.d.
	DMSO	347.5 (6.50 x 10^3), 492 (1.38 x 10^4)	542	0.0016 ± 0.0002
Ph_2P-CH_2-pip-NBD	$NCCH_3$	-	n.d.	n.d.
	DMSO	349 (9.05 x 10^3), 494 (2.65 x 10^4)	550	0.0096 ± 0.0005

.

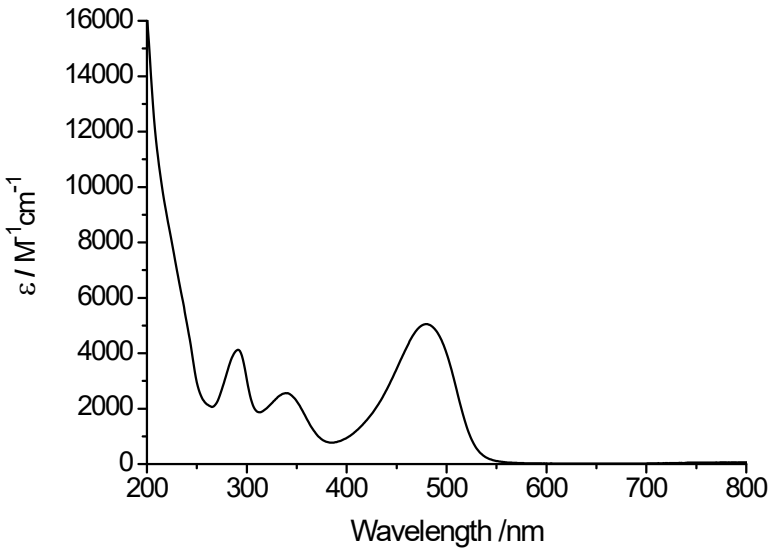

Figure S16. UV-Vis spectra of **1** in acetonitrile.

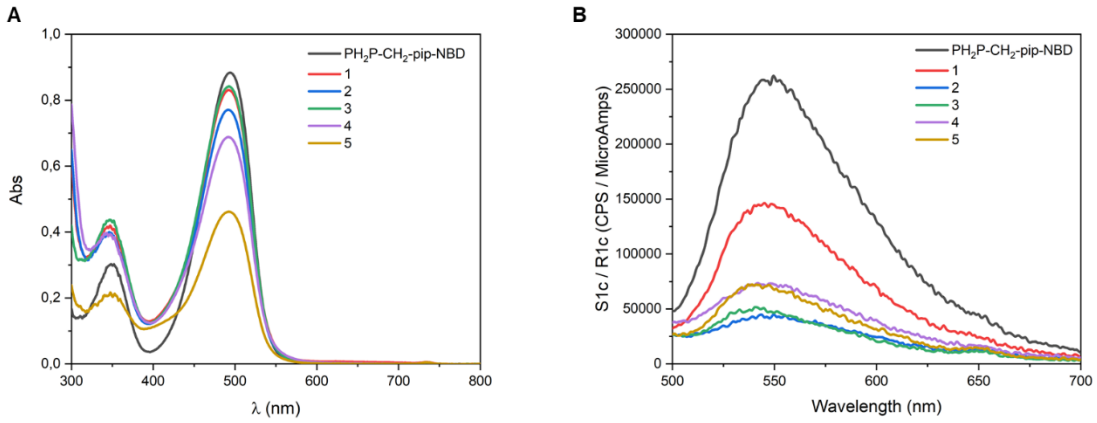

Figure S17. Absorption (**A**) and fluorescence (**B**) (λ_{exc} = 345 nm) spectra of complexes **1**–**5** and Ph_2P-CH_2-pip-NBD in DMSO. Absorption spectra were obtained from 10^{-3} M solutions.

S3. X-ray crystallographic structure determination

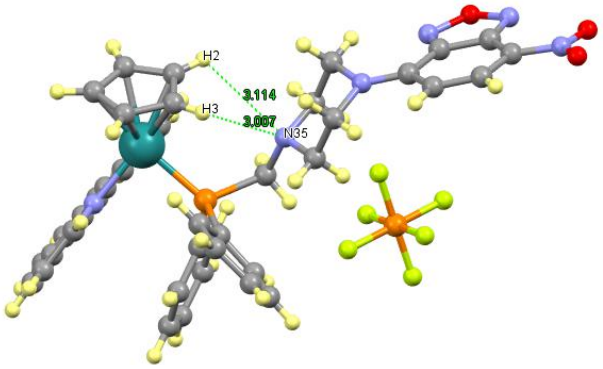

Figure S18. Intramolecular hydrogen bonds for compound **5.**

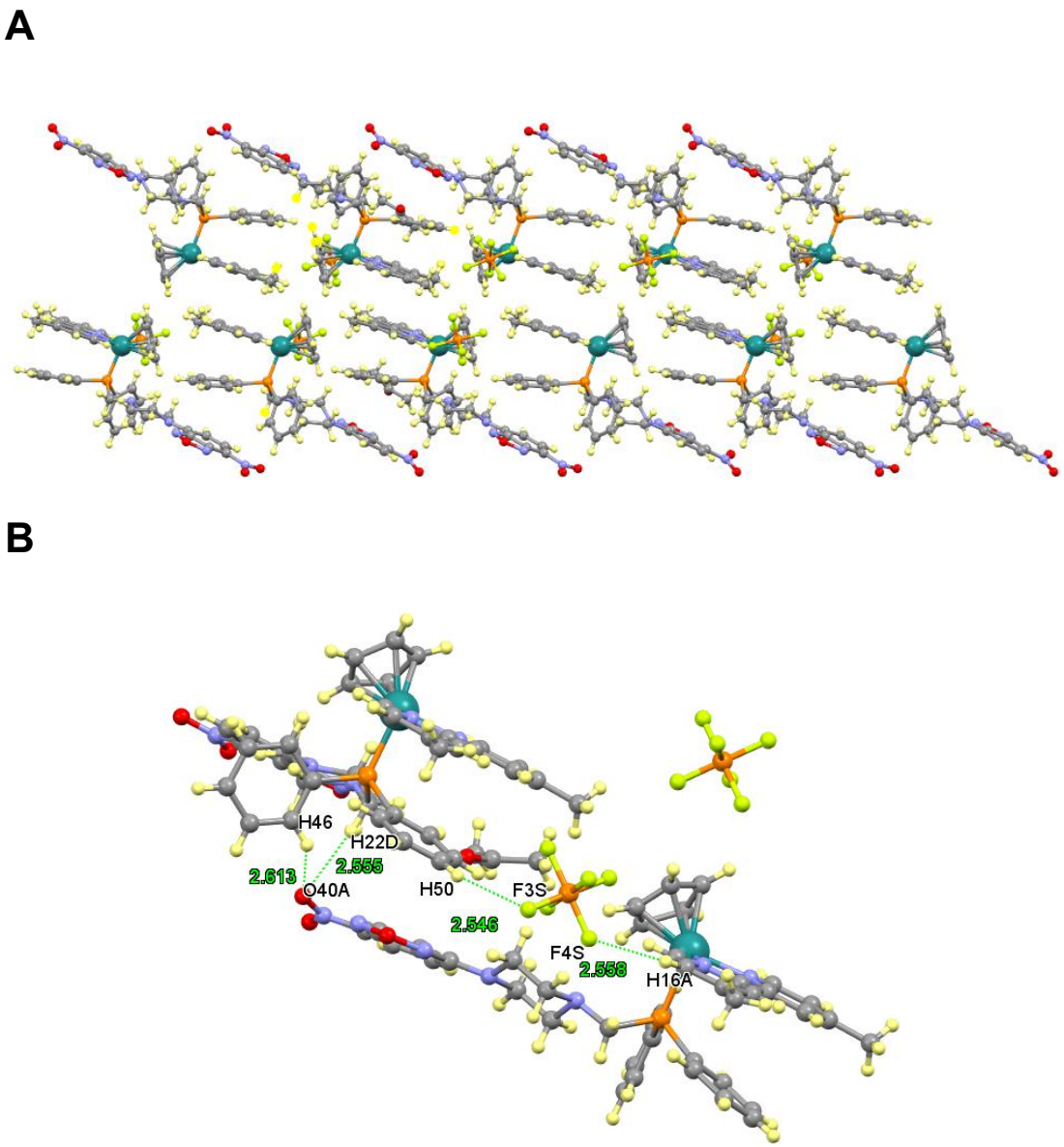

Figure S19. Packing diagram along *a* axis (**A**) and intermolecular hydrogen bonds (**B**) for compound **1.**

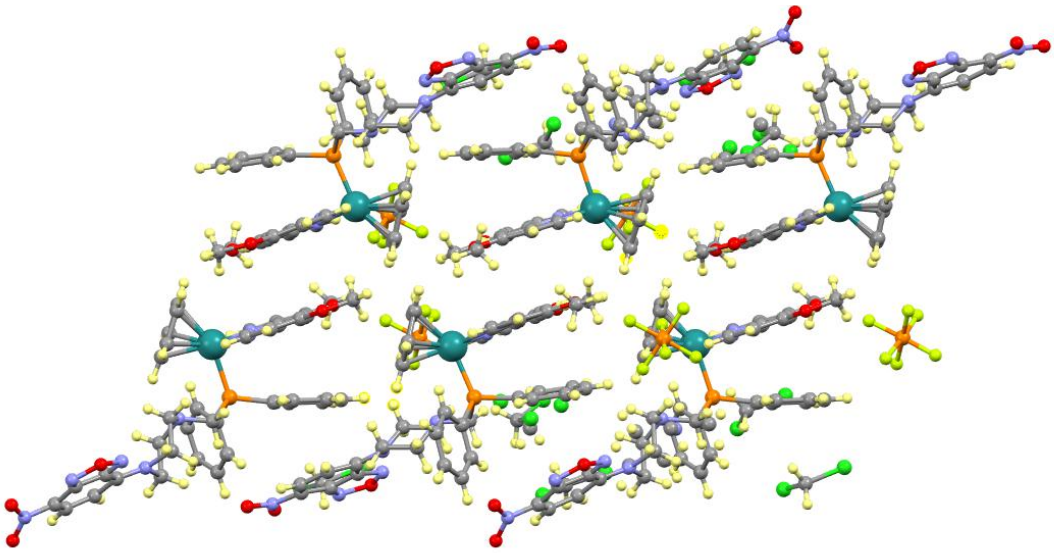

Figure S20. Packing diagram along *a*-axis for compound **3**.

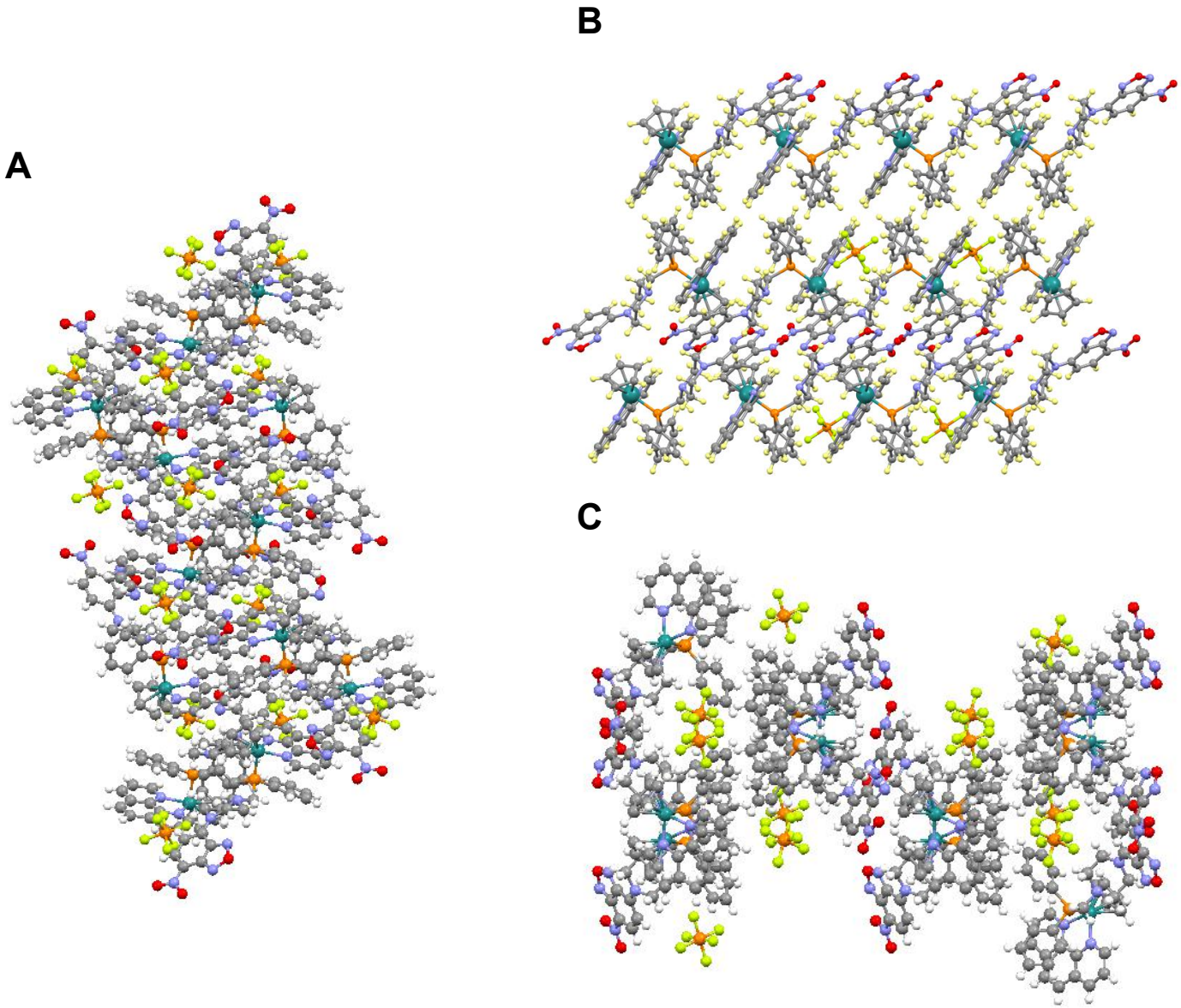

Figure S21. Packing diagram along *a*-axis (**A**), *b*-axis (**B**) and *c*-axis (**C**) for compound **5**.

S4. Stability studies in aqueous solution

i) Stability studies by ^{1}H and $^{31}P\{^{1}H\}$ NMR spectroscopy in 100% DMSO-d_6.

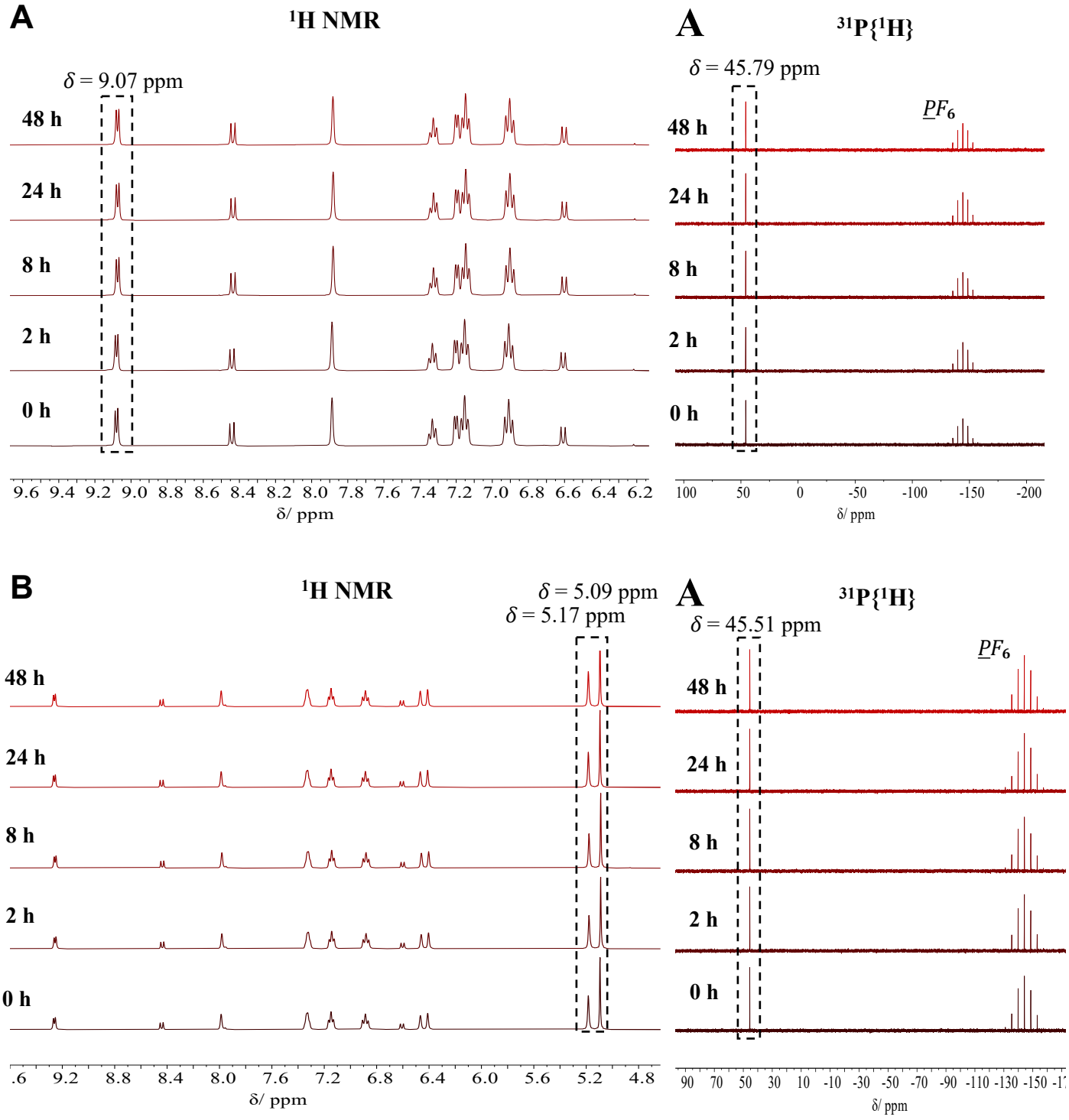

Figure S22. Stability studies in DMSO-d_6 for complex **1** (**A**) and complex **4** (**B**) followed by ^{1}H- and $^{31}P\{^{1}H\}$-NMR spectroscopy during 48 h. No changes were detected confirming that the complexes remained unchanged over 24 hours.

ii) Stability studies by UV-Vis spectroscopy in 5% DMSO / 95 % DMEM

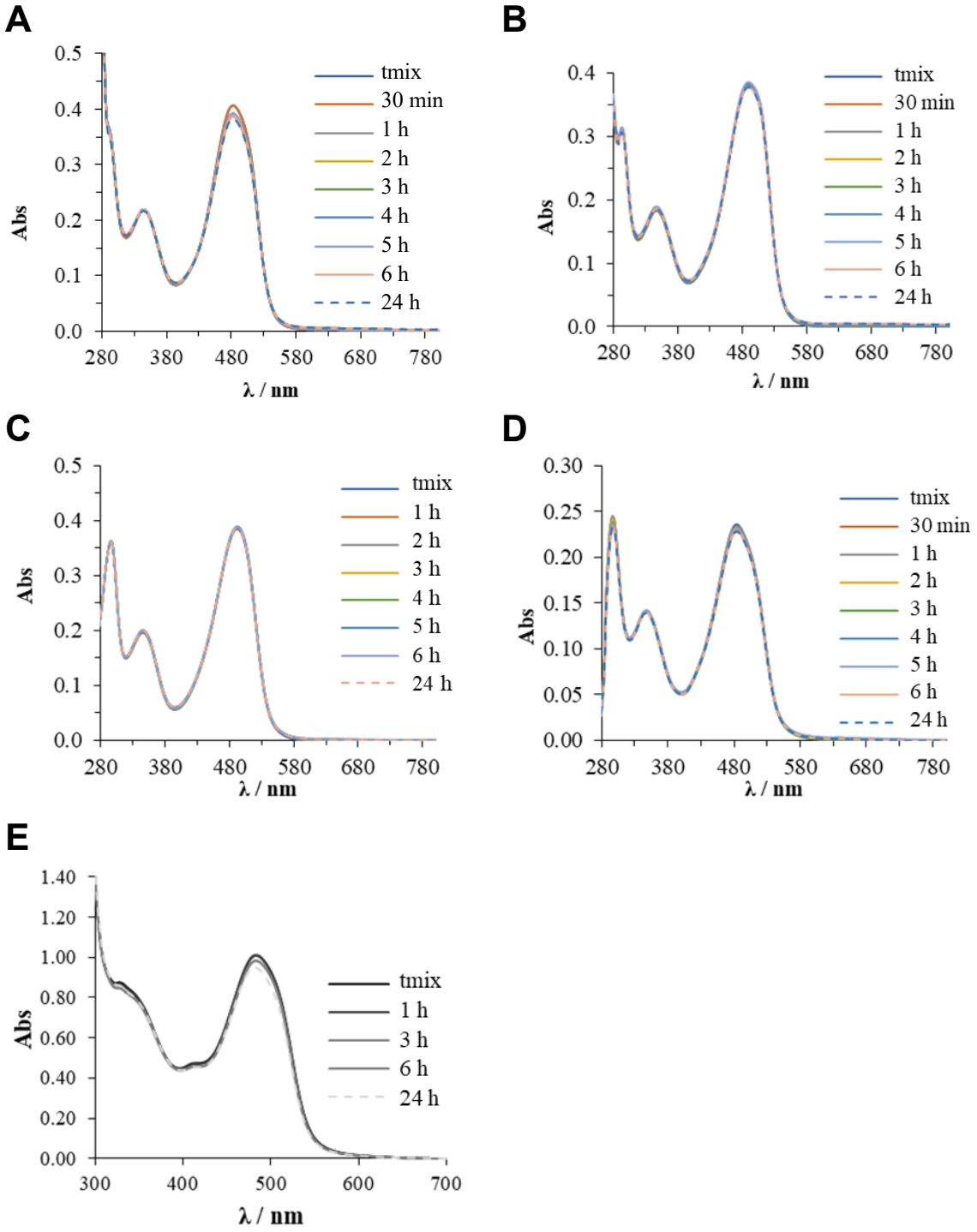

Figure S23. Stability studies in cellular media (5% DMSO / 95 % DMEM) for complexes **1** (**A**), **2** (**B**), **3** (**C**), **4** (**D**), and **5** (**E**) followed by UV-Vis spectroscopy over a 24 h period (1 cm optical path; see experimental section for details).

S5. Biological activity data

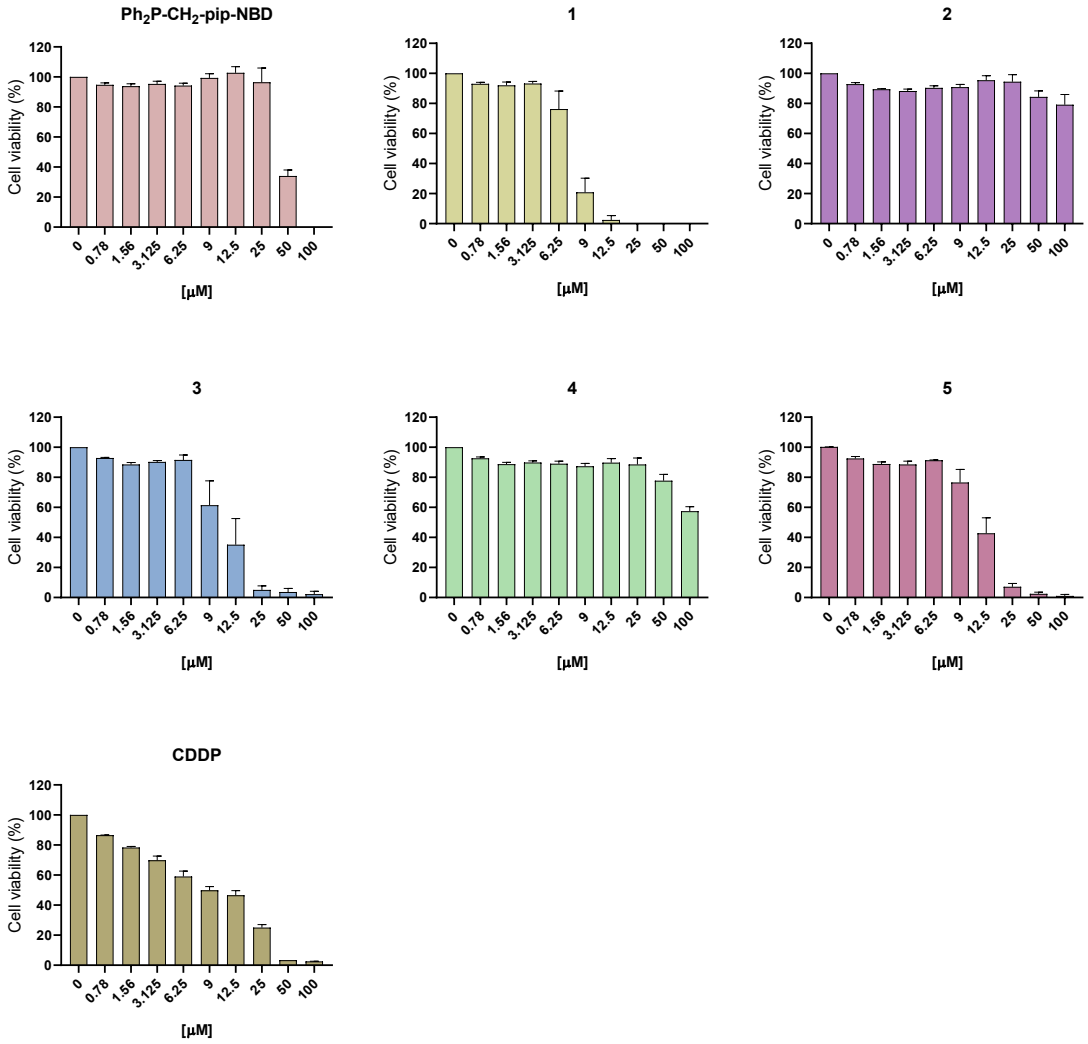

Figure S24. Cytotoxicity of Ph_2P-CH_2-pip-NBD, complexes **1**–**5**, and cisplatin (CDDP) on 4T1 cells upon 48 h of incubation. The data are expressed as means ± standard error of the mean (SEM) for 2-3 experiments.

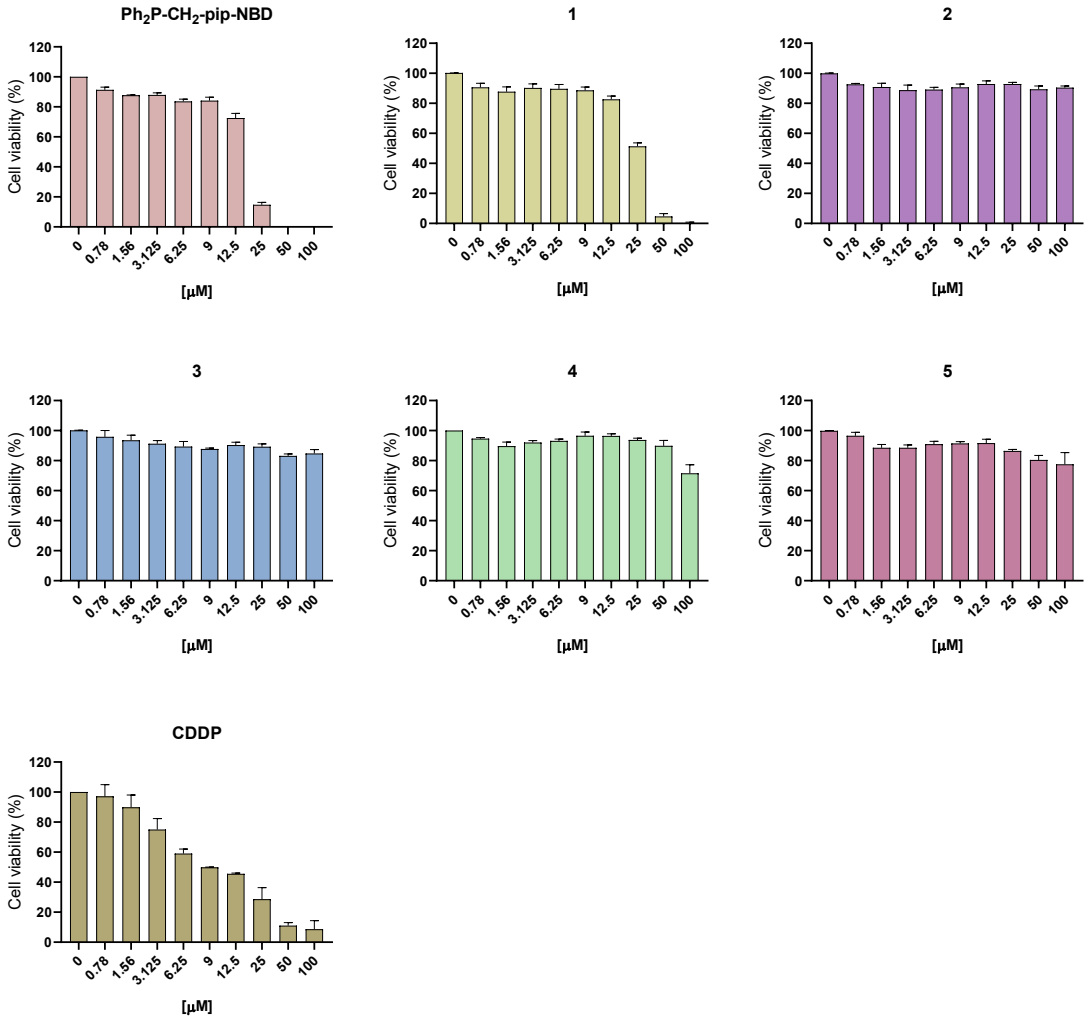

Figure S25. Cytotoxicity of Ph_2P-CH_2-pip-NBD, complexes **1**–**5**, and cisplatin (CDDP) on CT26 cells upon 48 h of incubation. The data are expressed as means ± standard error of the mean (SEM) for 2-3 experiments.

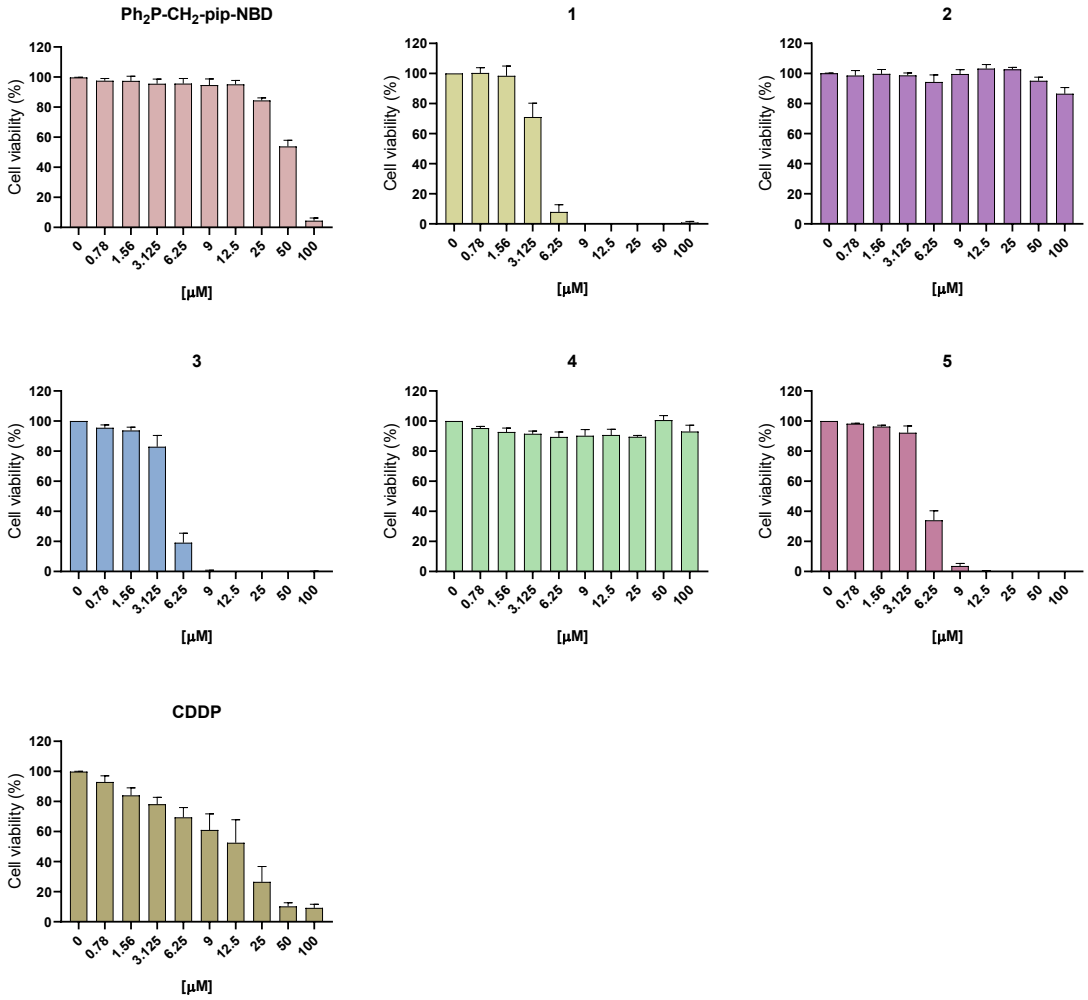

Figure S26. Cytotoxicity of Ph_2P-CH_2-pip-NBD, complexes **1**–**5**, and cisplatin (CDDP) on U2OS cells upon 48 h of incubation. The data are expressed as means ± standard error of the mean (SEM) for 3 experiments.

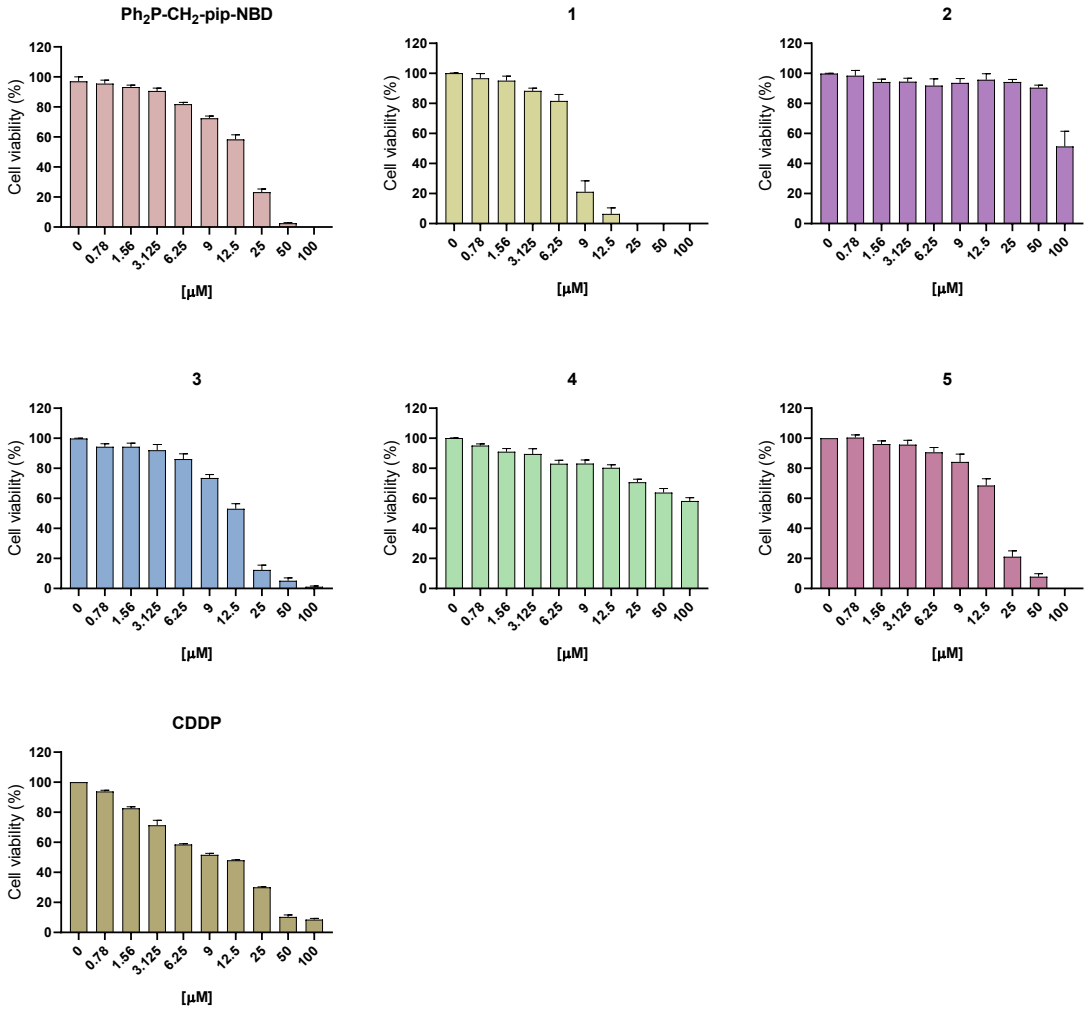

Figure S27. Cytotoxicity of Ph_2P-CH_2-pip-NBD, complexes **1**–**5**, and cisplatin (CDDP) on 3T3 cells upon 48 h of incubation. The data are expressed as means ± standard error of the mean (SEM) for 2-3 experiments.

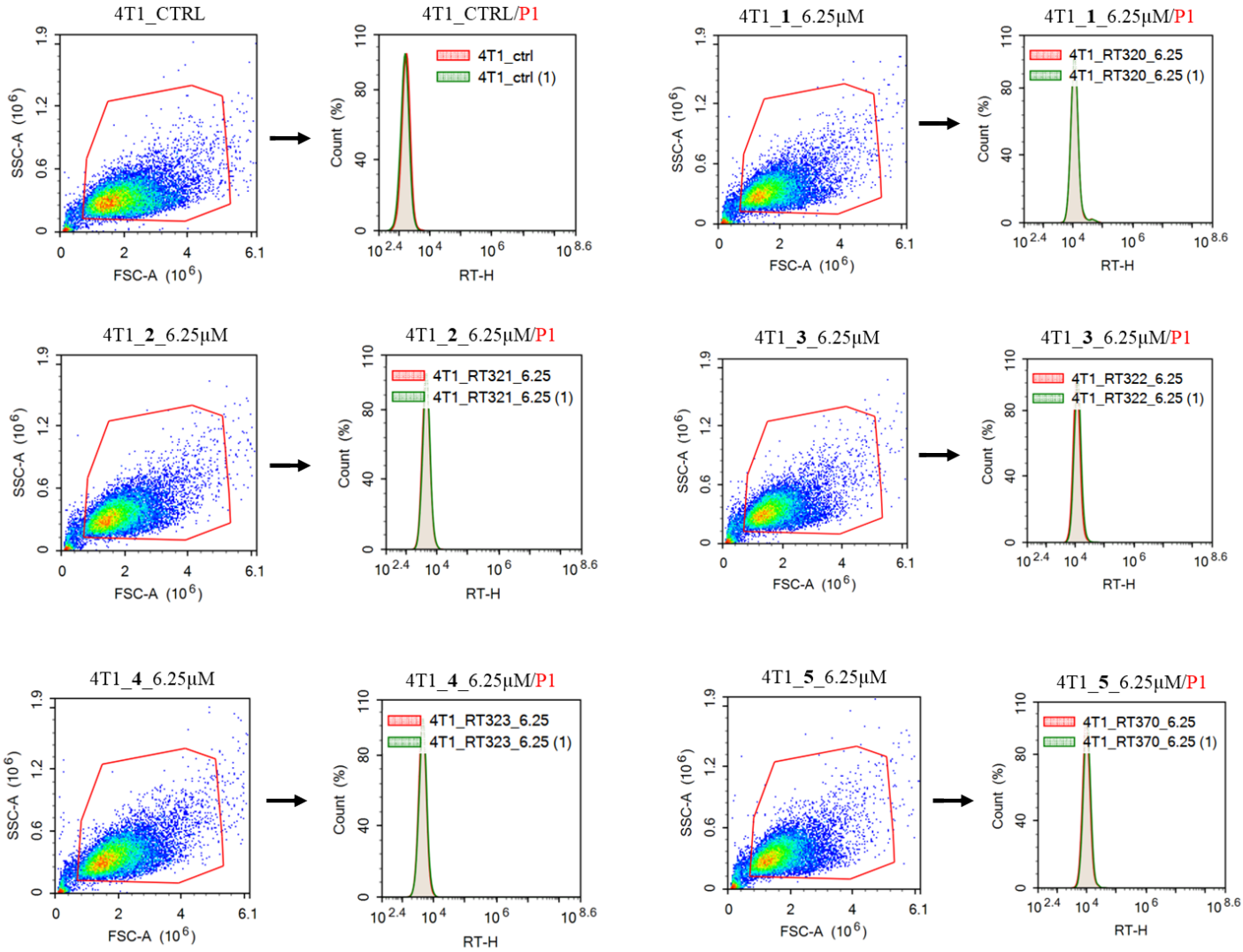

Figure S28. Scatter plot (Gating) and histogram of flow cytometry data. The representative histograms show the distribution of the fluorescence intensity of the compounds at a concentration of 6.25 μM for the selected population, following 25 hours incubation in 4T1 cells. In the histograms, RT320, RT321, RT322, RT323, and RT370 correspond to compounds **1**, **2**, **3**, **4**, and **5**, respectively.

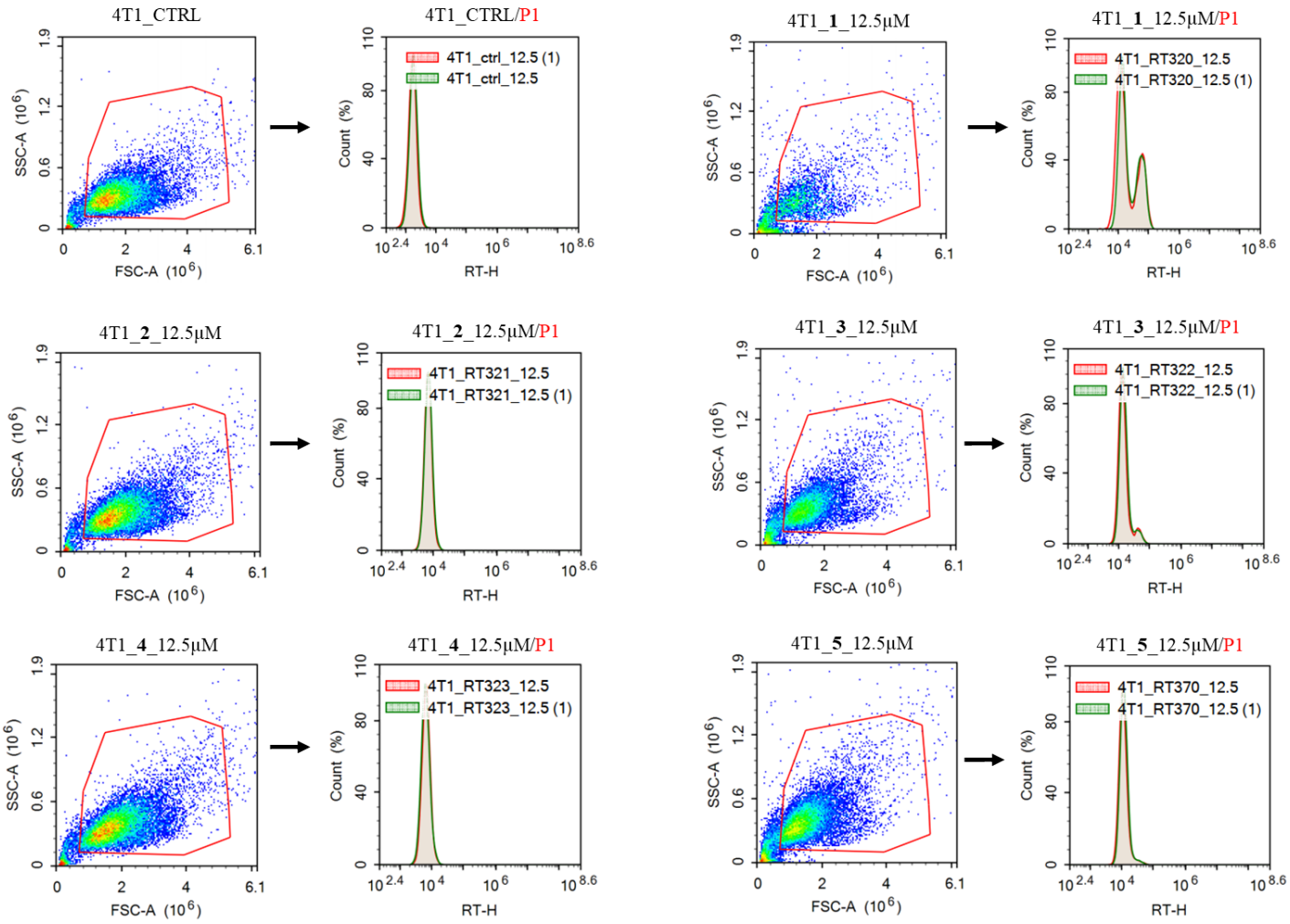

Figure S29. Scatter plot (Gating) and histogram of flow cytometry data. The representative histograms show the distribution of the fluorescence intensity of the compounds at a concentration of 12.5 μM for the selected population, following 25 hours of treatment of 4T1 cells. In the histograms, RT320, RT321, RT322, RT323, and RT370 correspond to compounds **1**, **2**, **3**, **4**, and **5**, respectively.

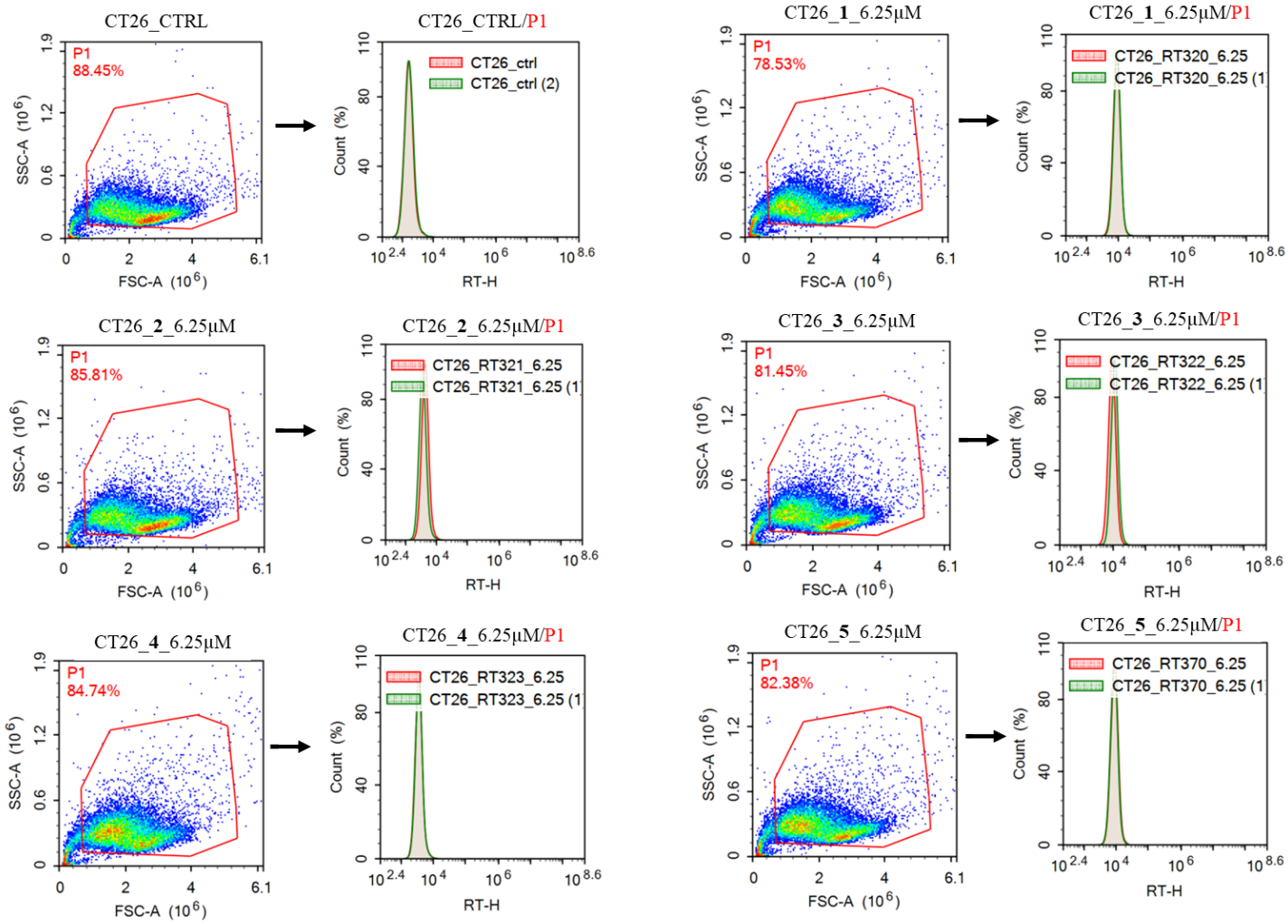

Figure S30. Scatter plot (Gating) and histogram of flow cytometry data. The representative histograms show the distribution of the fluorescence intensity of the compounds at a concentration of 6.25 μM for the selected population, following 25 hours of treatment of CT26 cells. In the histograms, RT320, RT321, RT322, RT323, and RT370 correspond to compounds **1**, **2**, **3**, **4**, and **5**, respectively.

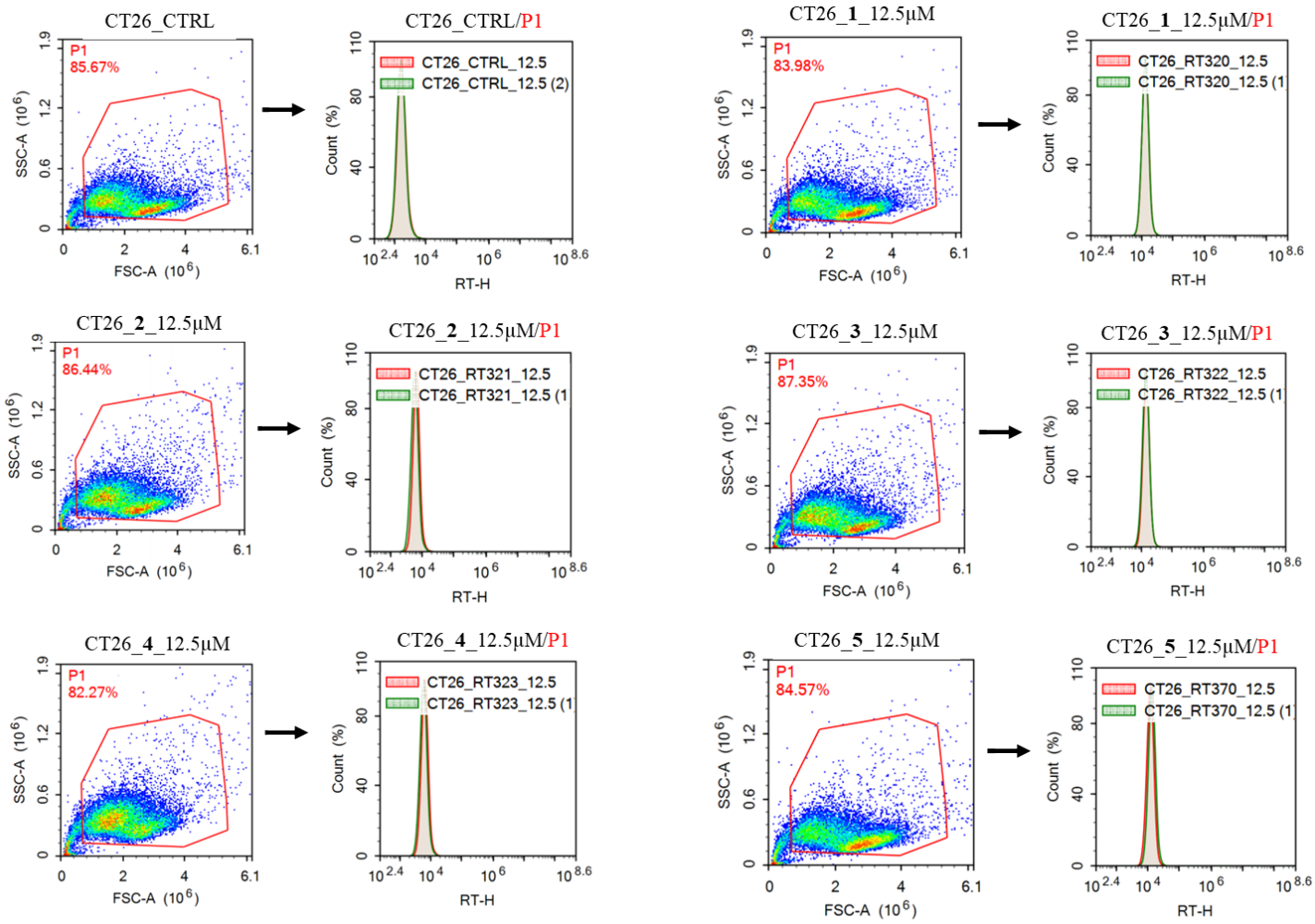

Figure S31. Scatter plot (Gating) and histogram of flow cytometry data. The representative histograms show the distribution of the fluorescence intensity of the compounds at a concentration of 12.5 μM for the selected population, following 25 hours of treatment of CT26 cells. In the histograms, RT320, RT321, RT322, RT323, and RT370 correspond to compounds **1**, **2**, **3**, **4**, and **5**, respectively.

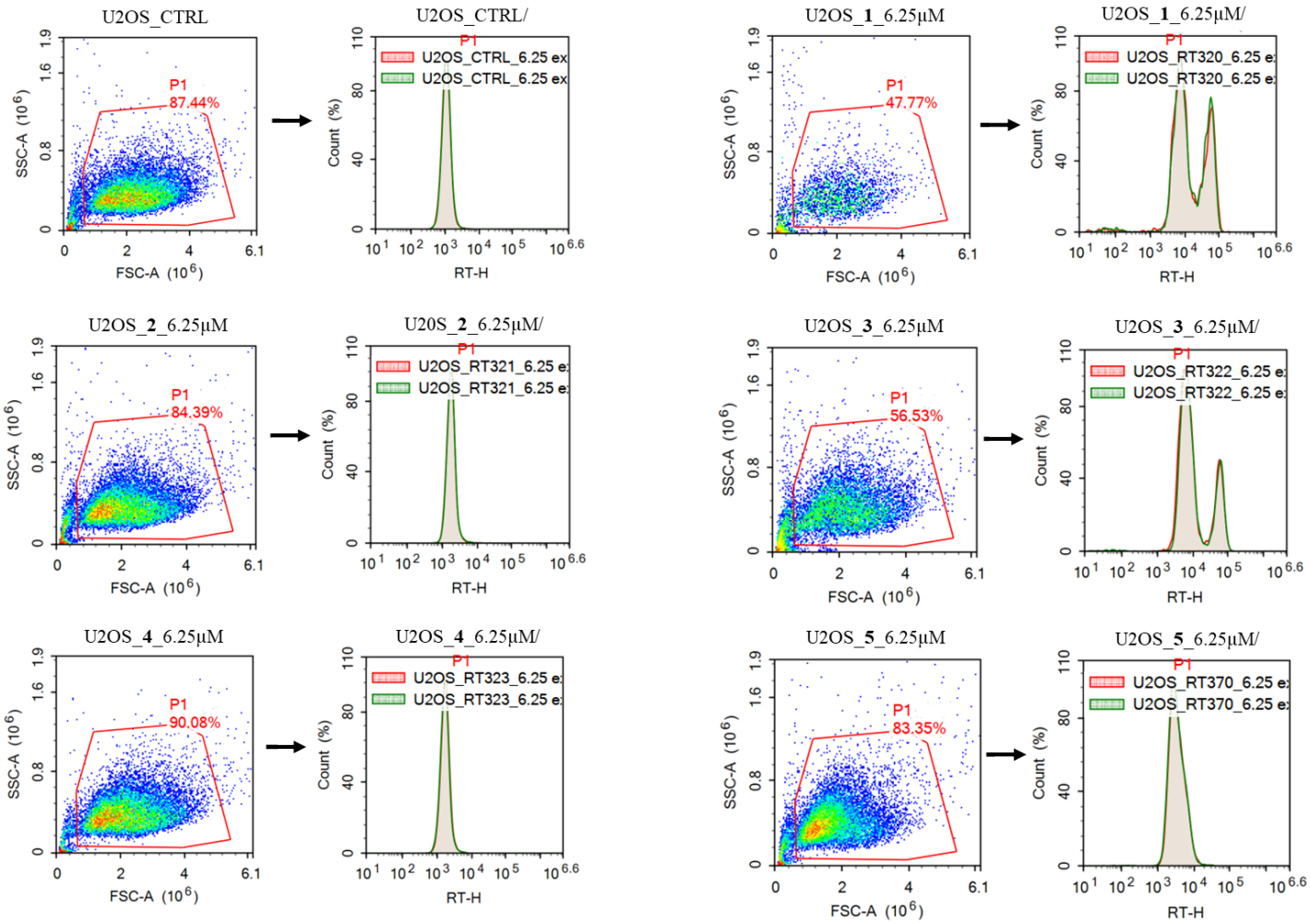

Figure S32. Scatter plot (Gating) and histogram of flow cytometry data. The representative histograms show the distribution of the fluorescence intensity of the compounds at a concentration of 6.25 µM for the selected population, following 25 hours of treatment of U2OS cells. In the histograms, RT320, RT321, RT322, RT323, and RT370 correspond to compounds **1**, **2**, **3**, **4**, and **5**, respectively.

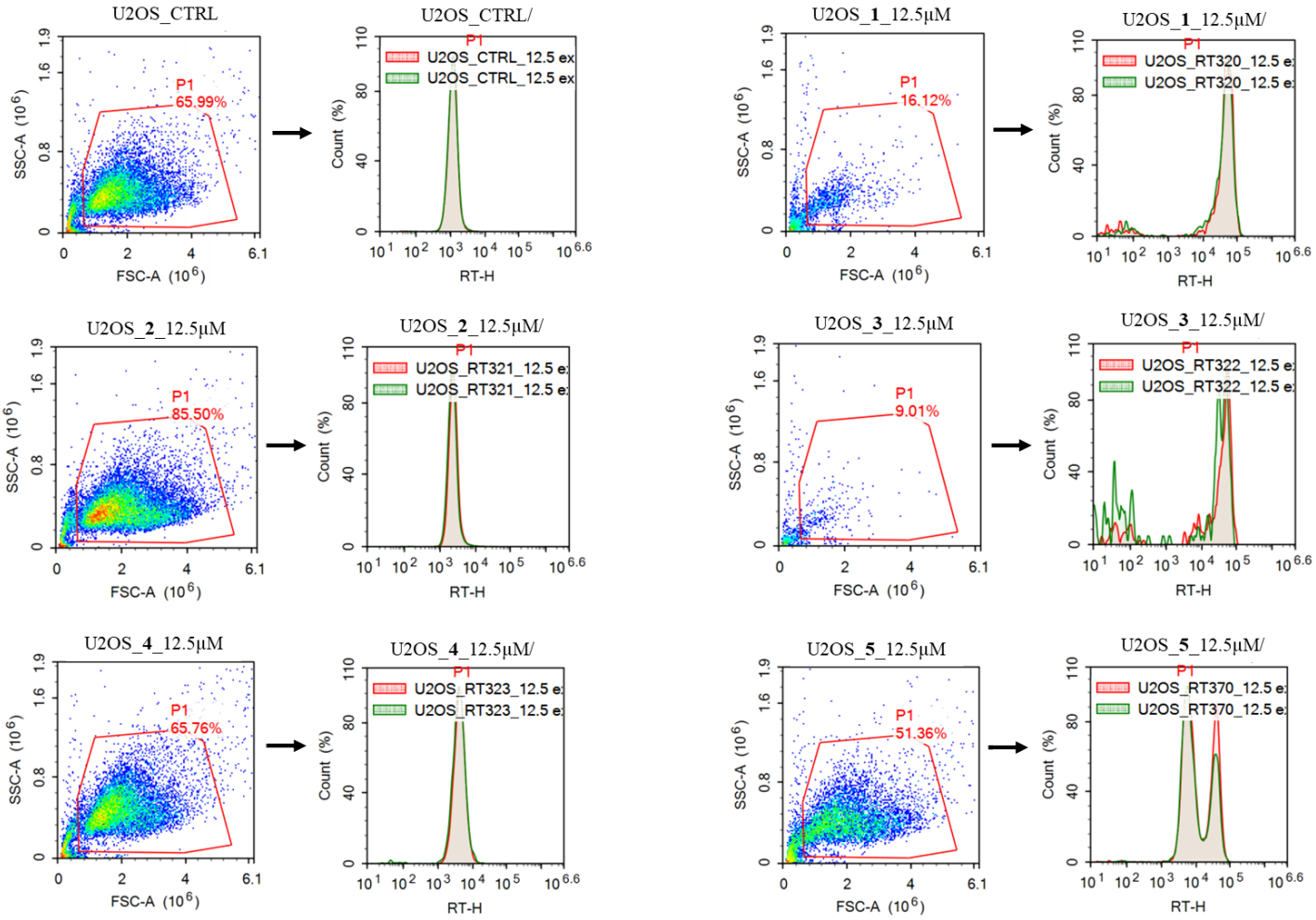

Figure S33. Scatter plot (Gating) and histogram of flow cytometry data. The representative histograms show the distribution of the fluorescence intensity of the compounds at a concentration of 12.5 µM for the selected population, following 25 hours of treatment of U2OS cells. In the histograms, RT320, RT321, RT322, RT323, and RT370 correspond to compounds **1**, **2**, **3**, **4**, and **5**, respectively.

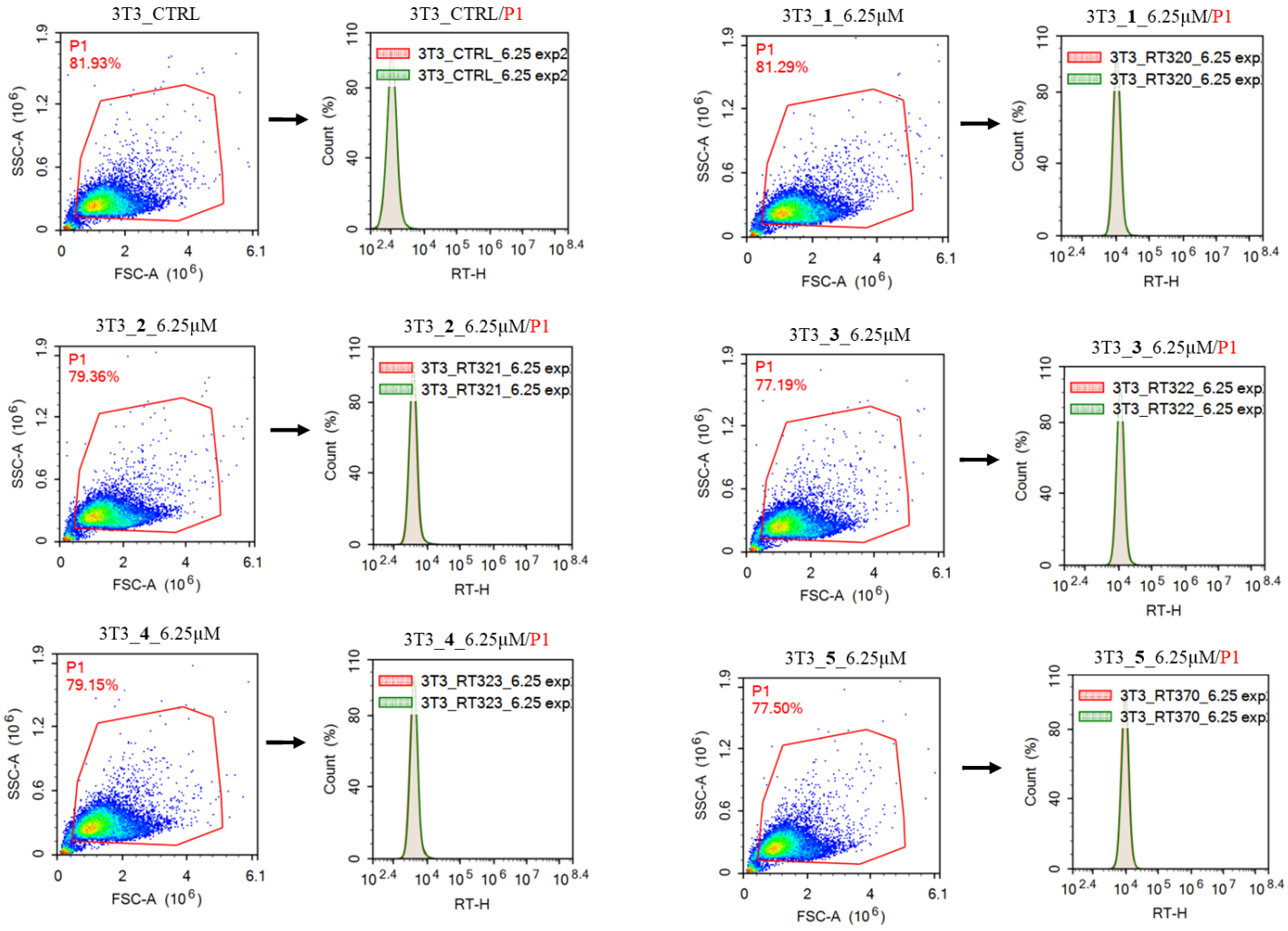

Figure S34. Scatter plot (Gating) and histogram of flow cytometry data. The representative histograms show the distribution of the fluorescence intensity of the compounds at a concentration of 6.25 µM for the selected population, following 25 hours of treatment of 3T3 cells. In the histograms, RT320, RT321, RT322, RT323, and RT370 correspond to compounds **1**, **2**, **3**, **4**, and **5**, respectively.

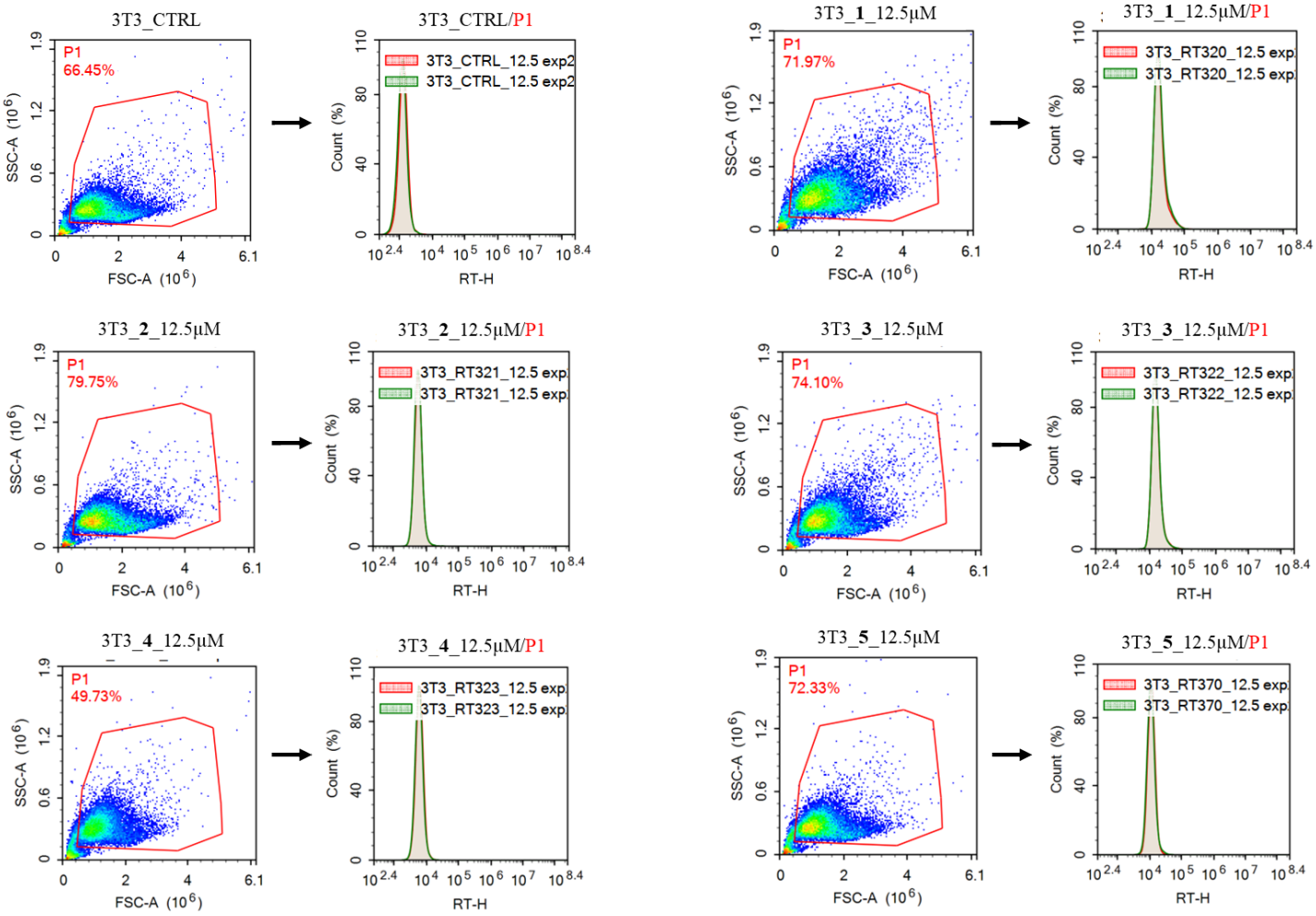

Figure S35. Scatter plot (Gating) and histogram of flow cytometry data. The representative histograms show the distribution of the fluorescence intensity of the compounds at a concentration of 12.5 μM for the selected population, following 25 hours of treatment of 3T3 cells. In the histograms, RT320, RT321, RT322, RT323, and RT370 correspond to compounds **1**, **2**, **3**, **4**, and **5**, respectively.

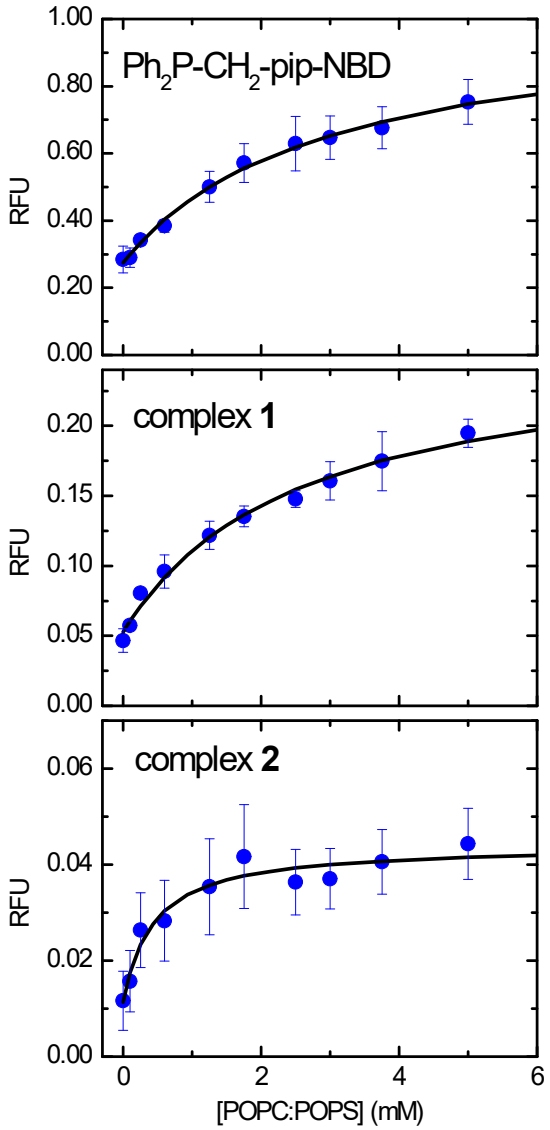

Figure S36. Fluorescence variation due to partition of Ph_2P-CH_2-pip-NBD (top), complex **1** (middle) and complex **2** (bottom) between an aqueous solution, pH 7.4, and POPC:POPS bilayers at 37 ºC. The fluorescence intensity (RFU) is relative to that of Ph_2P-CH_2-pip-NBD when fully associated with the membrane, note the different scales of the y-axis that reflect the relative fluorescent quantum yield of the compounds when associated with the membrane. The points represent experimental values (mean from 4–8 experiments ± standard deviation), while the line corresponds to the best fit of equation (1), with LogK_p values of 2.54 ± 0.23 (for Ph_2P-CH_2-pip-NBD), 2.76 ± 0.26 (for complex **1**), and 3.42 ± 0.35 (for complex **2**), respectively.

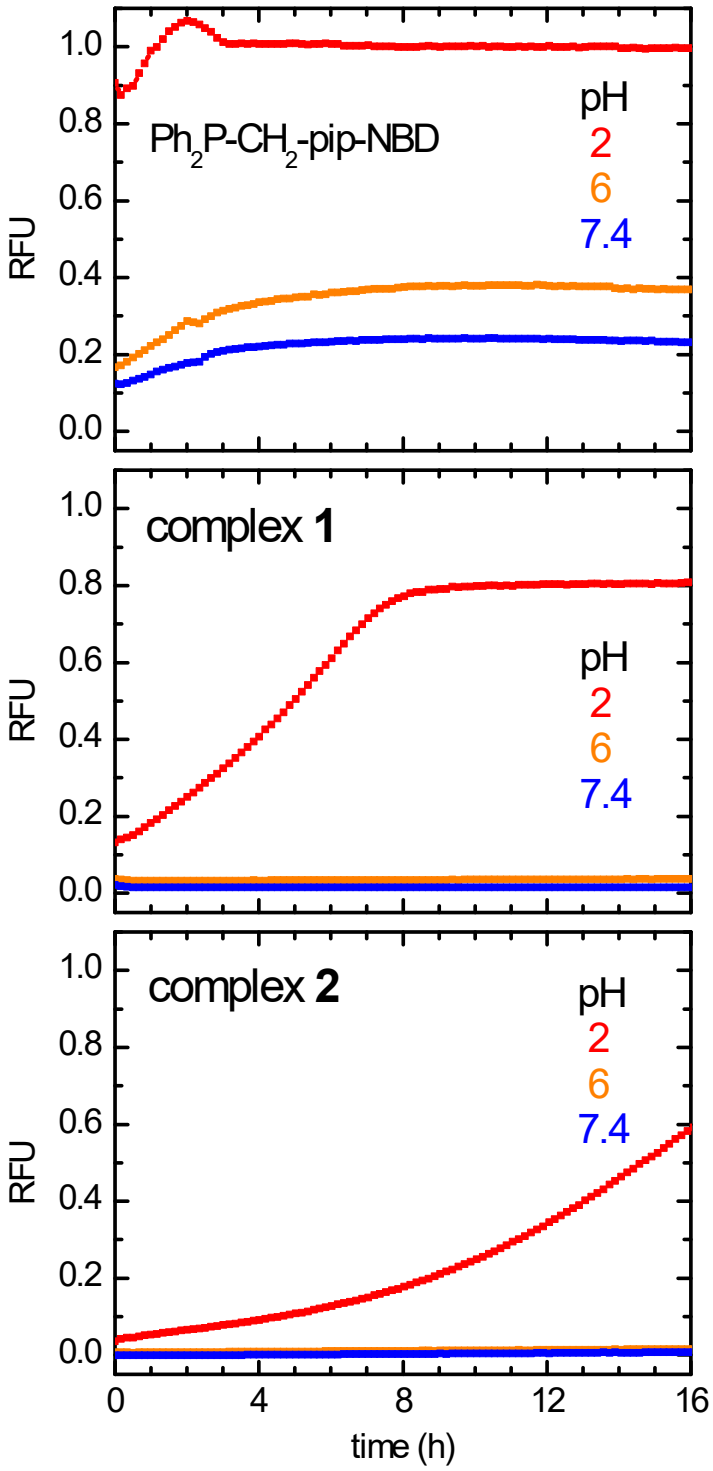

Figure S37. Fluorescence variation of Ph_2P-CH_2-pip-NBD (top), complex **1** (middle), and complex **2** (bottom) when incubated at the pH values indicated. The y axis is the fluorescence intensity relative to that of Ph_2P-CH_2-pip-NBD at pH=2, with excitation at 440 nm and fluorescence emission collected at 550 nm for all.

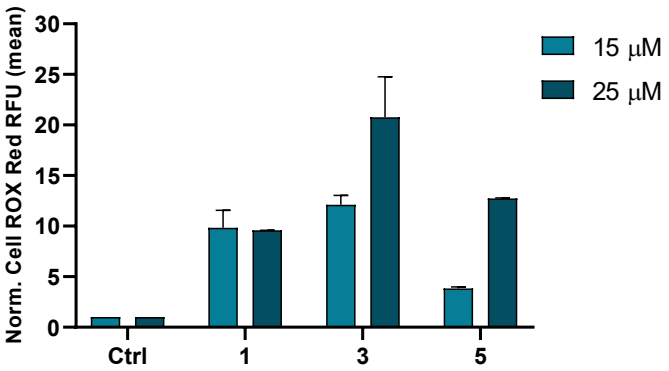

Figure S38. Oxidative stress in 4T1 cells treated with compounds **1**, **3**, and **5** for 6 hours, evaluated using CellROX® Deep Red (5 μM). Bars represent the mean ± SEM of two independent experiments.

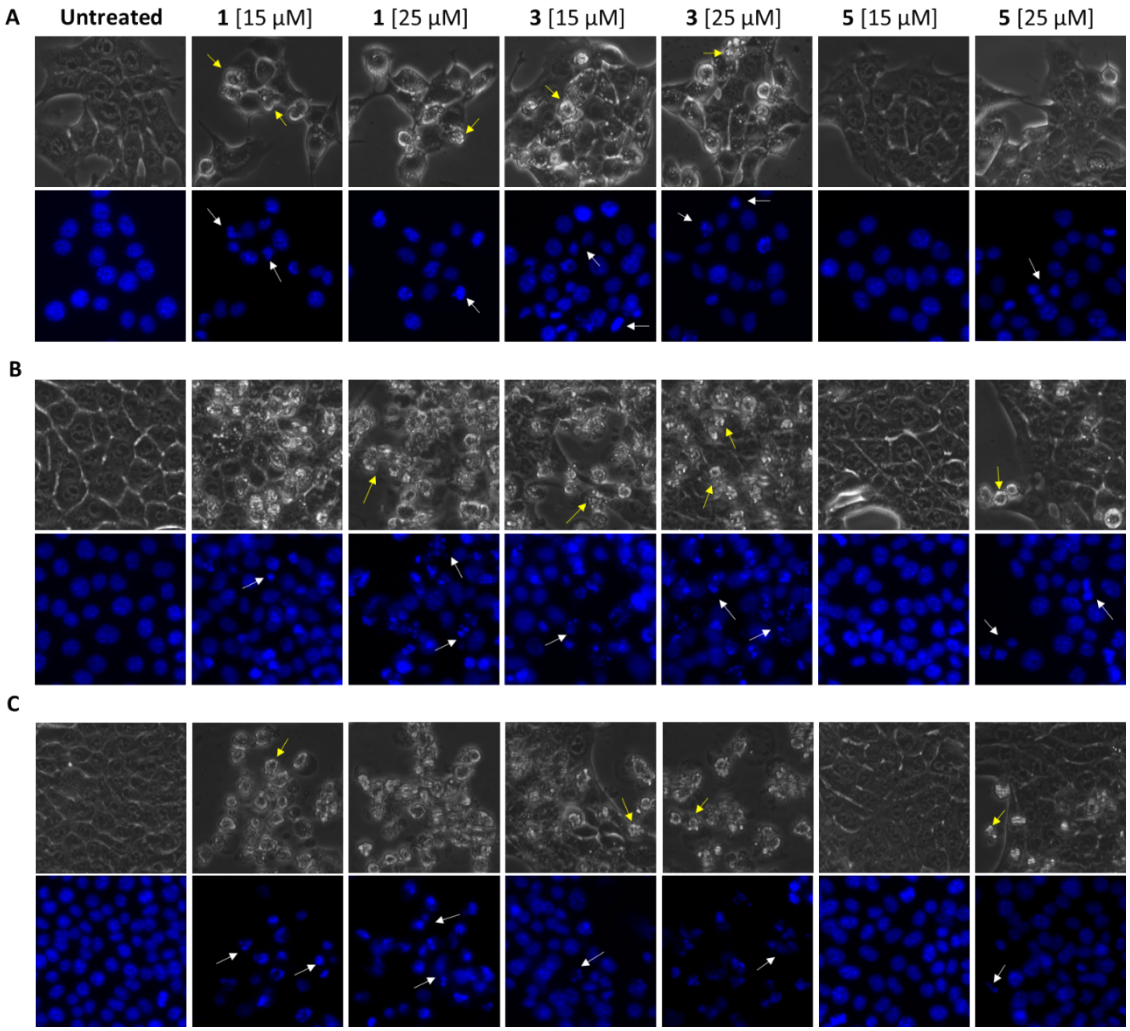

Figure S39. Representative images of 4T1 cells incubated with compounds **1**, **3**, and **5** (15 and 25 µM) for (**A**) 6 h, (**B**) 24 h, and (**C**) 48 h. Yellow arrows indicate apoptotic bodies in the brightfield images, while white arrows highlight chromatin condensation and fragmentation visible upon Hoechst staining (blue). Images are representative of two independent experiments. Magnification: 20×.